Abrikosov dislocation lattice in a model of the cholesteric–to–smectic-A transition

S. R. Renn
Department of Physics, Loomis Laboratory, University of Illinois–Urbana-Champaign, 1110 West Green Street, Urbana, Illinois 61801

T. C. Lubensky
Department of Physics, University of Pennsylvania, Philadelphia, Pennsylvania 19104-6396
(Received 7 March 1988)

The nematic–to–smectic-A transition in liquid crystals is analogous to the normal to superconducting transition in metals with the Frank director $\mathbf{n}$ in liquid crystals playing the role of the vector potential $\mathbf{A}$ in metals. The liquid-crystal analog of an external magnetic field is a field, arising, for example, from molecular chirality, leading to a nonzero $\nabla\times\mathbf{n}$ in the equilibrium nematic phase. The cholesteric (twisted nematic) phase is the analog of a normal metal in an external magnetic field. In type-II superconductors in an external magnetic field, the Abrikosov flux lattice phase with partial flux penetration intervenes between the low-temperature Meissner phase and the high-temperature normal-metal phase. In this paper we study the analog in liquid crystals containing chiral molecules of the Abrikosov phase in superconductors. Using a covariant form of the de Gennes free energy, we find that in mean-field theory a state, which we call the twist-grain-boundary (TGB) state, with regularly spaced grain boundaries consisting of parallel screw dislocations, intervenes between the smectic and cholesteric phases. We calculate the liquid-crystal analogs of the upper and lower critical fields H_{c2} and H_{c1}. The properties of the TGB phase depend on the angle $2\pi\alpha$ between axes of dislocations in adjacent grain boundaries. α can be rational or irrational. When $\alpha=p/q$ for mutually prime integers p and q, the TGB state has a q-fold screw axis and quasicrystalline symmetry for crystallographically forbidden q. Our calculations ignore exponentially small terms favoring lock in at rational α. We calculate the x-ray scattering intensities in the cholesteric phase near the TGB phase boundary and in the TGB phase for rational and irrational α. We also discuss experimental difficulties in observing the TGB state and the possible effects fluctuations not included in mean-field theory might have on its existence.

I. INTRODUCTION

The nematic–to–smectic-A transition[1] is, perhaps, the best known and most extensively studied of the phase transitions occurring in liquid crystals. One of the primary notions that has emerged from these studies is the close analogy between this transition and the normal to superconducting transition in metals.[2,3] The basis of this analogy is simple: the ordered phases of both smectics-A and superconductors are characterized by a nonvanishing complex order parameter ψ. For a superconductor, the order parameter is the complex gap function whereas for the smectic, it is the complex amplitude of the periodic modulation of the nematogen density. Furthermore, the coupling in smectics between ψ and $\delta\mathbf{n}$, the deviation of the director $\mathbf{n}$ from some position-independent average orientation, $\mathbf{n}_0$, is identical to that between the gap function and the vector potential in a superconductor. The analogy can be pushed further since the spatial average of the twist $\mathbf{n}\cdot(\nabla\times\mathbf{n})$ corresponds to the magnetic induction $\mathbf{B}$. The field h thermodynamically conjugate to the average twist then corresponds to the magnetic intensity $\mathbf{H}$. Thus, the cholesteric (or twisted nematic) is the analog of a normal metal in an external magnetic field. The expulsion of twist occurring at the cholesteric–to–smectic-A transition is then the liquid-crystal analog of the Meissner effect. These analogies can be made quite precise by comparing the de Gennes free-energy functional for the smectic[2] with the Landau-Ginzburg free energy for a superconductor.[4,5]

Yet the analogy between smectics and superconductors is incomplete in that, at the time of this writing, no analog of the Abrikosov[6,5] flux lattice has been found in smectics. Superconductors are characterized by the ratio, κ (the Ginzburg parameter), of their penetration depth λ to their coherence length ξ. They are classified as type-I superconductors if $\kappa<1/\sqrt{2}$ and type-II if $\kappa>1/\sqrt{2}$. The Abrikosov flux lattice occurs only in type-II systems. Thus one explanation of the absence of a vortex lattice analog in liquid crystals could be that all smectic liquid crystals are type-I. This explanation, however, contradicts our current (albeit incomplete) understanding of the nematic–to–smectic-A transition. In type-I systems, fluctuations drive the second-order mean field normal-to-superconducting transition first order.[7] In type-II systems, however, fluctuations are believed to lead to a second-order transition in the universality class of the inverted xy model.[8] The nematic–to–smectic-A transition is observed to be second order in a large number of materials.[9] On the basis of the analogy with superconductors, one would argue that these materials are type-II and should, therefore, have the analog of an Abri-

kosov phase when chiral molecules are added. To the authors' knowledge, there has been no direct determination of the Ginzburg parameter for liquid crystals.

The subject of this paper is the putative Abrikosov phase in type-II smectic liquid crystals. Such a phase, if it exists, would consist of a network of screw dislocations. Sethna[10] has argued, however, that a spatially infinite set of parallel dislocations with nonzero areal density n_A is impossible. His argument is as follows: Define u to be the smectic layer displacement and consider a circular contour of radius R lying in a plane perpendicular to the dislocation lines as shown in Fig. 1. The contour will enclose an area containing $\pi R^2 n_A$ dislocations. Therefore, $\int dl \cdot \nabla u = (\pi R^2 n_A) d$ where d is the smectic layer spacing. This implies that the average of $|\nabla u|$ over the contour is equal to $\frac{1}{2} R d n_A$ and grows without bound as $R \to \infty$. In other words, the slope of the smectic planes relative to a fixed plane perpendicular to the axis of the dislocations diverges as $R \to \infty$ indicating that such a configuration does not have a well-defined thermodynamic limit. We are, therefore, forced to consider a more complex dislocation network.

We will show that, to a very good approximation, the minimum energy dislocation network consists of a regular array of parallel twist grain boundaries composed of regularly spaced parallel twist dislocations with axes that rotate from one grain boundary to the next. We call this the twist-grain-boundary (TGB) state. Figure 2 shows a schematic representation of the cholesteric phase with its pitch axis parallel to the x axis and the TGB state into which it transforms. Note the similarity of the direction

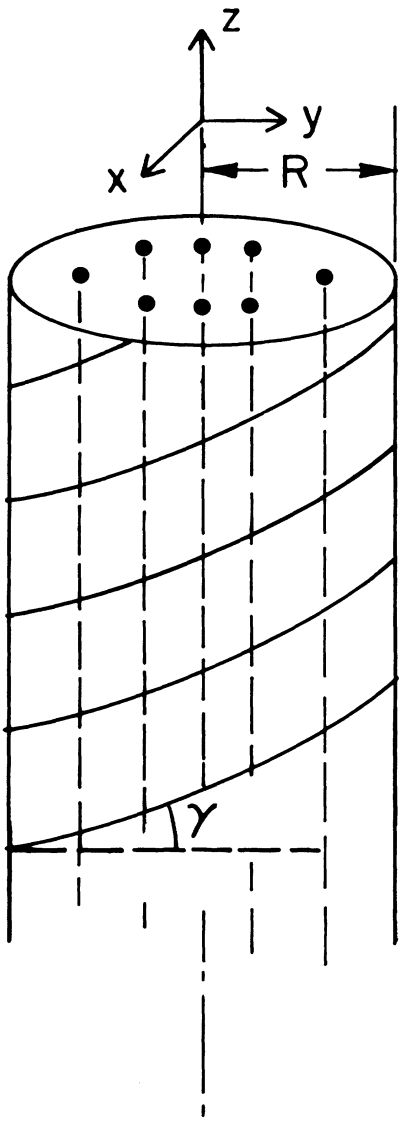

FIG. 1. Schematic representation of a circular area C of radius R in a smectic liquid crystal containing an average areal density n_A of screw dislocations with Burgers vector of magnitude d parallel to the z axis. The integral of u around the boundary of C is equal to $\pi n_A R^2 d$, the number of dislocations enclosed in C. Thus $|\nabla u| = \tan\gamma$ on the boundary of C is proportional to R, and the slope ot the smectic layers relative to the xy plane diverges as $R \to \infty$.

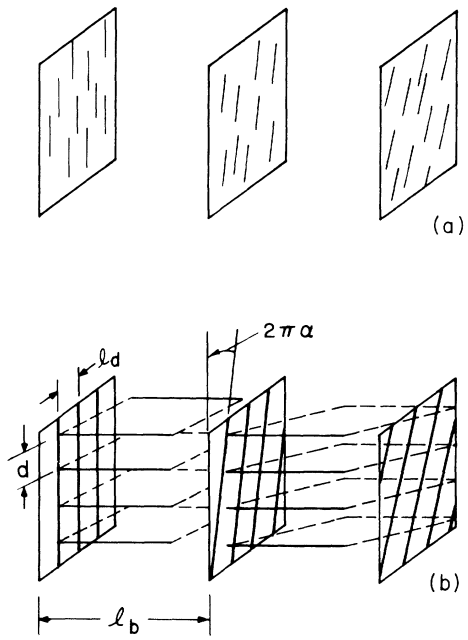

FIG. 2. (a) Schematic representation of a cholesteric liquid crystal. The director $\mathbf{n}(\mathbf{x}) = \mathbf{n}_0(x)$ lies in the (y,z) plane and rotates in a helical fashion as the coordinate x along the pitch axis increases. The director executes one full turn in a distance equal to the pitch $P = 2\pi/k_0$. (b) Schematic representation of the TGB state. There are regularly spaced twist grain boundaries separated by a distance l_b. Each grain boundary consists of regularly spaced screw dislocations (represented by dark lines) separated by a distance l_d. The axes of the dislocations in the nth grain boundary are at an angle $2\pi\alpha n$ with respect to the z axis. The configuration of molecules between grain boundaries is essentially identical to that of the low-temperature smectic-A phase with regularly spaced layers separated by a distance d. The angles of the normal to the smectic planes separated by a grain boundary differ by $\theta_0 = d/l_d$. Note that the average configuration of the director in the TGB phase is very similar to that of the cholesteric phase.

of molecular alignment in the two phases. Figure 3 shows why a plane of parallel twist dislocations constitute a twist grain boundary.

To arrive at our results, we use a covariant version[11] of the de Gennes model in an external magnetic field confining the director to planes[12] perpendicular to the cholesteric pitch axis. We calculate the upper and lower fields h_{c2} and h_{c1} by calculating, respectively, the limit of stability of the cholesteric phase and when it is first favorable to insert a single twist dislocation into the smectic-A phase. Near h_{c2}, we use an analysis similar to that of Abrikosov[6,13] for a superconductor to determine the properties of the TGB state.

The nature of the TGB state depends on the difference, $2\pi\alpha$, in angle between dislocation axes in adjacent grain boundaries. If α is irrational, the state is incommensurate along the pitch axis; if α is rational, it is commensurate along the pitch axis. When $\alpha=p/q$ is rational, the structure has a q-fold screw axis. If this screw axis is not crystallographically allowed (i.e., if $q\neq 2,3,4,6$), then the TGB state has quasicrystalline[14–16] rather than periodic crystalline symmetry and is incommensurate in the plane perpendicular to the pitch axis. Our calculations ignore exponentially small terms in the free energy that might lock-in rational values of α. Our mean-field phase diagram, therefore, looks identical to that for a superconductor as shown in Fig. 4(a). When neglected terms are included, a phase diagram such as that shown in Fig. 4(b) might result. Because of the anisotropy of the Frank elastic constants, there are also metastable TGB states in type-I smectics for which there is no analog in superconductors.

Information about the spatial structure of any phase is contained in its x-ray scattering intensity $I(\mathbf{q})$ at wave vector $\mathbf{q}$. We calculate $I(\mathbf{q})$ in the TGB phase and in the cholesteric phase just above h_{c2}. Our results are summarized in Fig. 5. If α is irrational, $I(\mathbf{q})$ in the TGB phase consists of a delta function cylinder parallel to the x axis of radius $q_0=2\pi/d$ and height ξ^{-1} where ξ is the smectic coherence length. When $\alpha=p/q$ is rational, $I(\mathbf{q})$ consists of delta function spikes on rings of radius q_0. In the cholesteric phase, $I(\mathbf{q})$ is a Lorentzian as a function of $q_\perp=(q_y^2+q_z^2)^{1/2}$ with a width tending to zero as $h\to h_{c2}$ and a Gaussian as a function of q_x with a width that remains finite at h_{c2}.

Our analysis is based entirely on mean-field theory. Fluctuations about the mean-field result may substantially alter our conclusions and may, in fact, lead to the disappearance of the TGB phase predicted by mean-field theory. The possible effects of fluctuations will be addressed in Sec. VIII.

This paper is organized as follows. Section II introduces the covariant constrained de Gennes model that is the basis of all of our calculations. Section III discusses the geometry of the TGB state. Section IV calculates the lower critical field h_{c1} and Sec. V the upper critical field h_{c2}. Section VI is an analysis of the TGB state near h_{c2}. Section VII calculates the x-ray scattering intensity $I(\mathbf{q})$ for the TGB and cholesteric states and compares this

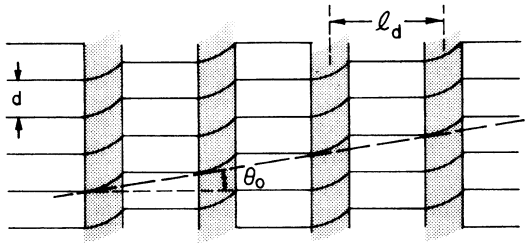

FIG. 3. Schematic representation of a twist grain boundary consisting of parallel twist dislocations (whose cores are darkened) of Burgers vector $d\hat{z}$ separated by distances l_d. The average slope relative to the y axis of the smectic planes in front of the grain boundary is $\frac{1}{2}d/l_d$ while the slope of those behind the grain boundary is $-\frac{1}{2}d/l_d$ leading to a change in angle of normals to smectic planes across the grain boundary of $\Delta\theta=2\tan^{-1}(\frac{1}{2}d/l_d)\sim d/l_d$.

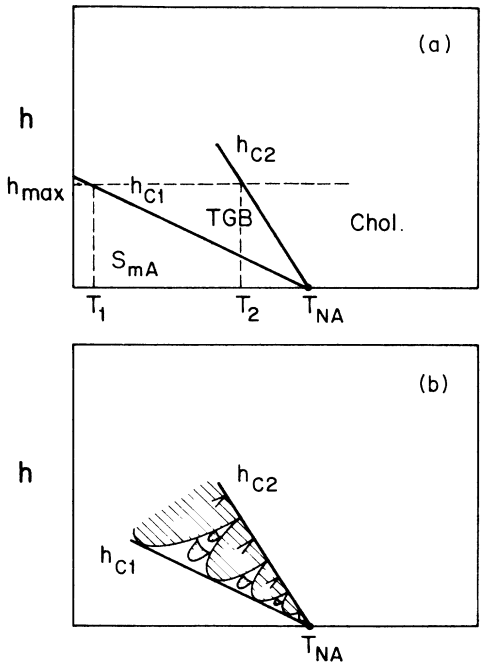

FIG. 4. Phase diagrams in the $h-T$ plane for liquid crystals doped with chiral molecules showing the cholesteric, smectic-A, and TGB phases. (a) Diagram obtained by the present calculations in which all exponentially small lock-in potentials are ignored. This phase diagram is identical to that of type-II superconductors. There is a single phase intervening between the high-temperature cholesteric and the low temperature smectic-A phase. The dashed horizontal line is the line $h=h_{max}$ where $h_{max}\approx K_2(2\pi/3000\ \text{Å})\approx 0.05$ dynes/cm is the maximum experimentally accessible value of h. The temperatures T_1 and T_2 are determined by $h_{max}=h_{c1}(T_1)=h_{c2}(T_2)$. (b) Hypothetical phase diagram of the type that might occur when lock-in terms in the model are included. There are tongues in the TGB region between h_{c1} and h_{c2} in which α locks in to a rational value. These tongues could be further divided into quasicrystalline regions and crystalline regions as discussed in the text. The positions and shapes of the lock-in regions are only schematic; they have not been calculated.

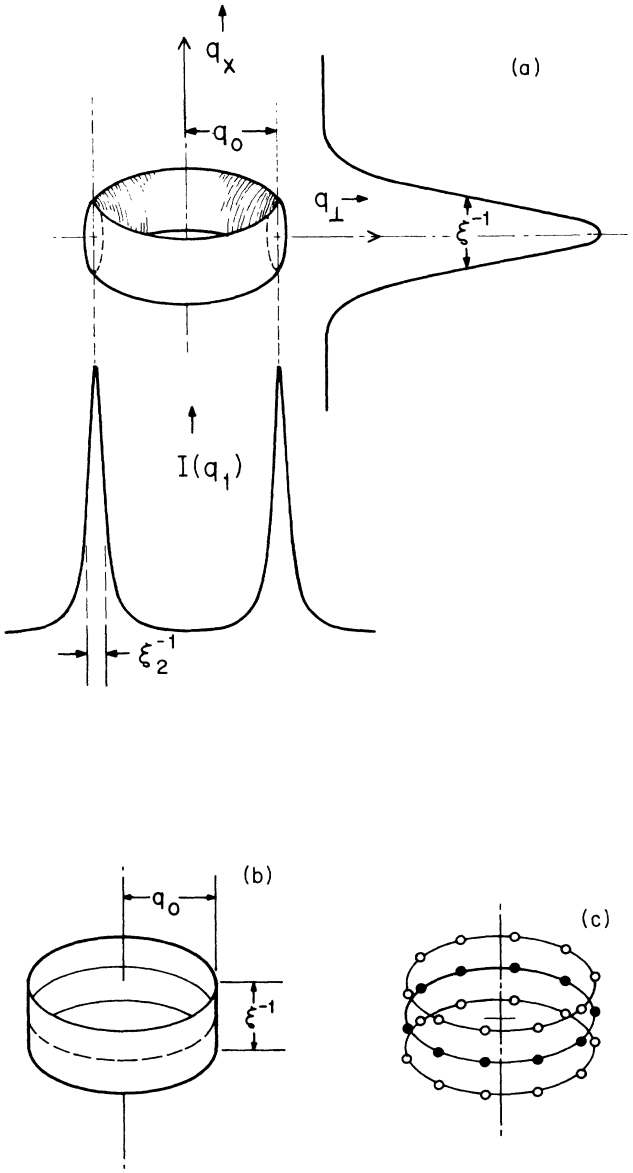

FIG. 5. X-ray scattering intensity $I(\mathbf{q})$ near h_{c2}. (a) $I(\mathbf{q})$ for the cholesteric phase just above h_{c2}. The scattering is intense on a torus obtained by rotating an oval centered at $q_z=q_0$ and $q_x=0$ about the q_x axis. As a function of q_x at fixed $\mathbf{q}_\perp$, $I(\mathbf{q})$ is a Gaussian of width $\bar{\xi}^{-1}\approx(q_0k_{c2})^{1/2}$. As a function of $q_\perp$ at fixed q_x, it is a Lorentzian of width ξ_2^{-1} [Eq. (5.12)]. In this figure the line shapes correspond to $k_{c2}=0.25q_0$, $\bar{\xi}^{-1}=0.5q_0$, and $\xi_x^{-1}=0.1q_0$. In experimental systems, $\bar{\xi}^{-1}$ is expected to be of order $0.1q_0$. (b) $I(\mathbf{q})$ in the TGB phase with α irrational. There is intense scattering on a cylinder of radius q_0 and height $\bar{\xi}^{-1}$. (c) $I(\mathbf{q})$ in the TGB phase with $\alpha=p/q$. There are Bragg peaks at equally spaced spots on rings of radius q_0 in the $y-z$ plane at $q_x=Jk_0/p$. If q is even, there are q spots in each ring; if q is odd, there are $2q$ spots in each ring. The intensity of the spots die off as $\exp(-q_x^2\xi^2)$. In this figure, only the Bragg peaks on rings at $q_x=0$ (closed circles) and $q_x\approx\bar{\xi}^{-1}$ (open circles) are drawn. There are actually $p\bar{\xi}^{-1}/k_{c2}\approx 10p$ rings between the two drawn in detail in the upper half plane. These are indicated as dotted rings.

function with powder and mosaic averaged functions with which it might be confused. Finally, Sec. VIII summarizes our results, reviews what has been left out of our calculations, and discusses prospects for experimental observations of the TGB phase.

II. THE COVARIANT de GENNES MODEL

In this section we will introduce a reformulation of the de Gennes model suitable for describing situations in which the Frank director is not necessarily restricted to be nearly uniform in space. We begin with the Frank free energy[17,18] for a nematic,

$$F_F=\tfrac{1}{2}\int d^3x\{K_1(\nabla\cdot\mathbf{n})^2+K_2(\mathbf{n}\cdot\nabla\times\mathbf{n})^2 +K_3[\mathbf{n}\times(\nabla\times\mathbf{n})]^2\}\ , \tag{2.1}$$

where K_1, K_2, and K_3 are, respectively, the splay, twist, and bend elastic constants. In a cholesteric,[18] the above nematic free energy should be replaced by the free energy

$$G_F=F_F-K_2k_0\int d^3x(\mathbf{n}\cdot\nabla\times\mathbf{n})\ , \tag{2.2}$$

where $K_2k_0\equiv h$ is a field arising from the presence of chiral molecules favoring nonzero $\mathbf{n}\cdot(\nabla\times\mathbf{n})$. G_F clearly has a locally stable minimum with respect to variations of $\mathbf{n}$ corresponding to the cholesteric state with director

$$\mathbf{n}_0(\mathbf{x})=(0,\sin k_0x,\cos k_0x) \tag{2.3}$$

and $\mathbf{n}_0\cdot\nabla\times\mathbf{n}_0=k_0$.

The director free energy of Eq. (2.2) for the cholesteric is the analog of the magnetic Gibbs free energy[5] for a metal,

$$G=\int d^3x\left[\frac{1}{8\pi\mu}(\nabla\times\mathbf{A})^2-\frac{1}{4\pi}\mathbf{H}\cdot\nabla\times\mathbf{A}\right]\ , \tag{2.4}$$

where $\mathbf{A}$ is the vector potential, $\mathbf{H}$ the magnetic intensity, and μ the magnetic permeability of the metal. It is clear from Eqs. (2.2) and (2.4) that $\mathbf{n}$ is the analog of $\mathbf{A}$, K_2^{-1} the analog of $4\pi\mu$, and $h\equiv K_2k_0$ the analog of $\mathbf{H}$. The thermodynamic magnetic induction $\mathbf{B}$ is the average of $\nabla\times\mathbf{A}$ over the volume V of the sample. The analog of $\mathbf{B}$ in the cholesteric is the volume average,

$$\bar{k}_0=\frac{1}{V}\int d^3x\ \mathbf{n}\cdot\nabla\times\mathbf{n}\ , \tag{2.5}$$

of $\mathbf{n}\cdot\nabla\times\mathbf{n}$. $\bar{k}_0$ measures the average rotation rate to the director. In the cholesteric phase in mean field theory, k_0 and $\bar{k}_0$ are equal. The magnetic permeability is unity in most cases and is generally not regarded as a temperature dependent quantity. In liquid crystals, fluctuations cause K_2 to diverge. The field h is unaffected by fluctuations, and $\bar{k}_0=h/K_2$ goes to go to zero at the nematic–to–smectic-A (NA) transition.[19] This unwinding of the cholesteric helix as the NA transition is approached has, in fact, been used to measure[20] the divergence of K_2. We will reexamine the behavior of $\bar{k}_0$ in Sec. VIII and find that it does not go to zero as these naive arguments would suggest. In the mean-field study to be

presented in what follows, we will assume K_2 is independent of temperature.

As discussed in the Introduction, the order parameter for the smectic phase is the complex density wave amplitude $\tilde{\psi}$ at wave vector $\mathbf{q}_0=q_0\mathbf{n}_0$, where $\mathbf{n}_0$ is a spatially uniform director. The de Gennes free energy[2] describing the NA transition is normally expressed as a function of $\tilde{\psi}$ and $\delta\mathbf{n}=\mathbf{n}-\mathbf{n}_0$. This description is best for situations in which $\delta\mathbf{n}$ is small. For example, it is appropriate for treating the NA transition since the average director is uniform in both the nematic and smectic-A phases, and deviations of the local director from $\mathbf{n}_0$ are small. In the cholesteric phase, the equilibrium director is spatially nonuniform, twisting in a helical pattern as discussed above. It is therefore useful to introduce a covariant form of the de Gennes free energy better suited for situations with an arbitrary spatially varying director. To do this we write the deviation of the nematogen density $\rho(\mathbf{x})$ from its spatially uniform average ρ_0 as

$$\delta\rho(\mathbf{x})=\rho(\mathbf{x})-\rho_0=\psi(\mathbf{x})+\psi^*(\mathbf{x}) . \tag{2.6}$$

The smectic order parameter ψ is understood to have Fourier components with wave vectors of magnitude of order q_0. In the smectic-A phase, $\psi=\tilde{\psi}e^{i\mathbf{q}_0\cdot\mathbf{x}}$. The covariant de Gennes free energy[11] is

$$\begin{aligned}F_G&=\int d^3x\{r\,|\,\psi\,|^2+[(C_\parallel-C_\perp)n_in_j+C_\perp\delta_{ij}][(\nabla-iq_0\mathbf{n})_i\psi(\nabla+iq_0\mathbf{n})_j\psi^*]+\tfrac{1}{2}g\,|\,\psi\,|^4\}\\&=F_G^0+F_G^{NL} ,\end{aligned} \tag{2.7}$$

where F_G^0 is the part of F_G quadratic in ψ and F_G^{NL} the part quartic in $|\,\psi\,|$. It is easily verified that F_G is invariant under the transformations $\psi(\mathbf{x})\to\psi(R^{-1}\mathbf{x})$ and $\mathbf{n}(\mathbf{x})\to R\,\mathbf{n}(R^{-1}\mathbf{x})$ where R is an arbitrary rotation matrix. The usual form of the de Gennes free energy is regained by setting $\psi=\tilde{\psi}e^{iq_0\cdot\mathbf{x}}$ and $\mathbf{n}=\mathbf{n}_0+\delta\mathbf{n}$ in Eq. (2.7). The coefficient of $|\,\tilde{\psi}\,|^2$ in the de Gennes free energy is then r so that the mean-field NA transition occurs at $r=0$. Therefore,

$$r\sim T-T_{\rm NA} , \tag{2.8}$$

where $T_{\rm NA}$ is the mean-field NA transition temperature.

The interaction with an external magnetic field $\mathbf{H}$ is described by

$$F_{\rm ext}=-\tfrac{1}{2}(\chi_\parallel-\chi_\perp)(\mathbf{H}\cdot\mathbf{n})^2 , \tag{2.9}$$

where $\chi_\parallel$ and $\chi_\perp$ are, respectively, the magnetic susceptibilities for fields parallel and perpendicular to $\mathbf{n}$. Here we assume $\chi_\parallel<\chi_\perp$ so that alignment of the director perpendicular to $\mathbf{H}$ is favored.[12] We further take $\mathbf{H}=H\hat{x}$ to be parallel to the axis of the cholesteric pitch and consider the limit $H\to\infty$. In this case, the director is energetically confined to the (y,z) plane and can be parametrized by a single angle variable:

$$\mathbf{n}(\mathbf{x})=(0,\sin\theta(\mathbf{x}),\cos\theta(\mathbf{x})) . \tag{2.10}$$

This constraint will considerably simplify our analysis. It inhibits the Landau-Peierls destruction of long-range helical order[21] in the cholesteric phase and eliminates the symmetric double twist[22] configuration at the core of a twist dislocation in the smectic phase. We believe, however, that the qualitative predictions of this constrained model will be correct for the more realistic case with less severe constraints.

As a final simplification, we take $C_\parallel=C_\perp\equiv C$ and $K_1=K_3\equiv K$. Our model free energy is thus

$$\begin{aligned}G&=F_G^0+F_G^{NL}+G_F\\&=\int d^3x[r\,|\,\psi\,|^2+C\,|\,(\nabla-iq_0\mathbf{n})\psi\,|^2]+\tfrac{1}{2}g\int d^3x\,|\,\psi\,|^4\\&\quad+\tfrac{1}{2}\int d^3x[K(\nabla_\perp\theta)^2+K_2(\nabla_x\theta-k_0)^2-K_2k_0^2] ,\end{aligned} \tag{2.11}$$

where as before F_G^0 is the part of the free energy quadratic in ψ, F_G^{NL} the part proportional to $|\,\psi\,|^4$, and G_F the director Gibbs free energy depending now only on θ. The simple form of the term following K_2 results because $\mathbf{n}\cdot(\nabla\times\mathbf{n})=\nabla_x\theta$ if $\mathbf{n}(\mathbf{x})$ satisfies Eq. (2.10). In the cholesteric phase, $\psi=0$ and $\nabla_x\phi=k_0$ so that the free-energy density of the cholesteric phase is $-\frac{1}{2}K_2k_0^2=-h^2/K_2$. In the smectic phase $(\nabla-iq_0\mathbf{n})\psi=0$ and $|\,\psi\,|^2=(-r/g)$ so that its free-energy density is $-\frac{1}{2}r^2/g$. The thermodynamic critical field,[23]

$$h_c=(K_2r^2/g)^{1/2} , \tag{2.12}$$

obtained by equating these two energies is the analog of H_c in a superconductor. In mean-field theory, the critical value of k_0 corresponding to h_c is $k_c=(r^2/K_2g)^{1/2}$.

Two important lengths in the free energy of Eq. (2.9) are the correlation length,

$$\xi=(c/|\,r\,|)^{1/2} , \tag{2.13}$$

and the twist penetration depth,

$$\lambda_2=(2Cq_0^2\psi^2/K_2)^{-1/2}=q_0^{-1}(K_2g/2C\,|\,r\,|)^{1/2} . \tag{2.14}$$

The twist Ginzburg parameter is thus

$$\kappa_2=\frac{\lambda_2}{\xi}=\frac{1}{Cq_0}\left[\frac{gK_2}{2}\right]^{1/2} . \tag{2.15}$$

This is the exact analog of the Ginzburg parameter for a superconductor. As we shall see, it plays an essential role in determining the nature of the smectic-cholesteric phase diagram as a function of T and k_0. In particular, the transition from type-I to type-II behavior occurs at $\kappa_2 = 1/\sqrt{2}$.

III. THE TWIST-GRAIN-BOUNDARY STATE

A type-II superconductor in an external magnetic field undergoes a transition at the lower critical field H_{c1} from the Meissner phase with excluded magnetic flux to the Abrikosov phase[5] consisting of a lattice of linear vortices parallel to the applied field. Each vortex carries a quantum of flux Φ_0 so that the magnetic induction is simply $n_v \Phi_0$ where n_v is the number of vortices per unit area. The analog in a smectic with chiral molecules of a vortex in a superconductor is a screw dislocation. As pointed out by Sethna[10] and discussed in the Introduction, a lattice of parallel screw dislocations leads to a physically unacceptable state, and another candidate state must be sought.

In the superconductor, the magnetic field at the vortex cores points in the same direction as the applied field. In the smectic, one should look for a lattice of twist dislocations that produces, on average, the same twisted director structure as occurs in the cholesteric phase. The rate of rotation $\bar{k}_0$ of the director should, however, be slower than in the cholesteric phase, just as the magnetic induction in the Abrikosov phase is less than it is in the normal phase. The lattice of dislocations having this property becomes almost obvious when one realizes that the average director in the core of a twist dislocation is parallel to the axis of the dislocation. Thus, it is natural to construct planes of parallel twist dislocations whose axes rotate in a helical fashion as one passes from one plane to the next as shown in Fig. 2. Each plane is a twist grain-boundary separating smectic regions with different layer normals. We, therefore, refer to this state as the twist-grain-boundary (TGB) state. The parameters characterizing the TGB state are the distance l_d between dislocations in a layer, the distance l_b between grain boundaries, and the separation d between smectic layers. The average rotation rate $\bar{k}_0$ can be calculated with the aid of Fig. 3. A given smectic layer rises by a half layer spacing $(d/2)$ in a half circuit around each dislocation. Thus the difference $\Delta\theta$ in angle of smectic plane normals on the two sides of the grain boundary is $2\theta_0$ where $\tan\theta_0$ is the average rise of a given layer per unit length:

$$\Delta\theta = 2\theta_0 = 2\tan^{-1}(\tfrac{1}{2}d/l_d) \sim d/l_d \ , \tag{3.1}$$

where, in the final equation, we assume $d \ll l_d$. This is equivalent to the change in angle of dislocation axes from one grain boundary to the next. The average rate of increase in θ is then

$$\bar{k}_0 = \frac{1}{L}\int_0^L dx\, \nabla_x \theta = \frac{\Delta\theta}{l_b} = \frac{d}{l_d l_b} \ , \tag{3.2}$$

where we used Eq. (2.5) and $\mathbf{n}\cdot(\nabla\times\mathbf{n}) = \nabla_x\theta$ for $\mathbf{n}$ satisfying Eq. (2.10). There are an infinity of choices for l_d and l_b yielding the same value of $\bar{k}_0$ just as there are an infinity of vortex lattices yielding the same value of $\mathbf{B}$ in a superconductor.

The nature of the TGB lattice depends on whether $\Delta\theta \equiv 2\pi\alpha$ is a rational or an irrational multiple of 2π. We, therefore, write the angle of nth grain boundary as

$$\theta_n = 2\pi\alpha n \equiv (k/q_0)n \ , \tag{3.3}$$

where $k = q_0\Delta\theta = 2\pi/l_d$ is the wave number of the dislocation lattice in a grain boundary. If $\alpha = (q_0 l_d)^{-1}$ is irrational, the lattice is incommensurate along the x axis since there are no grain boundaries with precisely the same angle. If α is rational, i.e., $\alpha = p/q$ with p and q relatively prime integers, the lattice is commensurate along the x axis since it consists of regularly repeated unit cells containing q grain boundaries undergoing a total of p rotations of 2π. Such a lattice, however, has a q-fold screw axis. Only one-, two-, three-, four-, and sixfold screw axes are consistent with the existence of a regular periodic lattice.[24] All other values of q lead to spatial structures with quasicrystalline rather than crystalline symmetry.[16] Their associated reciprocal lattices have no shortest length vector and are thus incommensurate. Therefore, the TGB state with q not equal to one of the crystallographically accepted values is incommensurate in the (y,z) plane even though α is rational.

Vectors in any reciprocal lattice[16] in d dimensions can be expressed as arbitrary integral linear combinations of r vectors in a basis (r is the rank of the reciprocal lattice). In periodic crystals, $r \le d$ whereas in incommensurate and quasicrystals, $q \ge r > d$. The phases of exactly r mass density waves are not determined by an energy minimization procedure. These r independent phases lead to r elastic-hydrodynamic variables[25] of which d are the usual lattice displacement variables and $d-r$ are phason variables. The number of phason degrees of freedom grows linearly with q for large q. Irrational values of α can be constructed as limits of rational values in which p and q become infinite. Thus, there are an infinite number of phason degrees of freedom (or energetically undetermined phases) when α is irrational. These degrees of freedom are probably associated with an indeterminancy in the origin of the arrays of parallel screw dislocations in each grain boundary. A detailed discussion of the elasticity and hydrodynamics of TGB structures is beyond the scope of this article.

IV. THE LOWER CRITICAL FIELD

Now that we have a description of the TGB analog of the Abrikosov vortex lattice, we can calculate the lower critical field h_{c1} in much the same way as Abrikosov[6,5] calculated H_{c1} for a superconductor. In the smectic phase the de Gennes order parameter is $\tilde{\psi} = |\tilde{\psi}|\, e^{iq_0 u}$ where u is the layer displacement variable. The elastic free energy depending only on u and $\delta\mathbf{n}$ is then

$$F_{\rm el} = \int d^3x \tfrac{1}{2}[B(\nabla u - \delta\mathbf{n})^2 + K(\nabla_\perp\theta)^2 + K_2(\nabla_x\theta)^2] \ , \tag{4.1}$$

where $\delta\mathbf{n} = (0, \sin\theta, \cos\theta - 1)$ and $B = C|\tilde{\psi}|^2 q_0^2 = C|r|q_0^2/g$. When the number of dislocations per unit

area is small ($l_d l_b \to \infty$), F_{el} can be linearized[26] about $\theta=0$ so that $\delta\mathbf{n}\approx\theta\hat{y}$. With this approximation, the energy of dislocations can be calculated using standard procedures. Minimization of Eq. (4.1) with respect to u and θ yields

$$\frac{\delta F_{el}}{\delta u} = -B\nabla\cdot(\nabla u-\delta\mathbf{n}) ,$$
$$\frac{\delta F_{el}}{\delta\theta} = -(K\nabla_1^2+K_2\nabla_x^2)\theta - B(\nabla_y u-\theta) . \tag{4.2}$$

The integral of $\mathbf{v}=\nabla u$ around a contour enclosing a dislocation of strength n is nd, and

$$\nabla\times\mathbf{v}=\mathbf{m}=d\sum_\alpha n_\alpha\int\delta[\mathbf{x}-\mathbf{R}_\alpha(l)]dl_\alpha , \tag{4.3}$$

where $\mathbf{m}$ is the dislocation density and n_α and $\mathbf{R}_\alpha(l)$ are, respectively, the strength and position of dislocation line α. From Eqs. (4.2) and (4.3), it follows that

$$\mathbf{v}(\mathbf{q})=i\frac{\mathbf{q}\times\mathbf{m}}{q^2}+\mathbf{q}\frac{q_y\theta}{q^2} ,$$
$$[q^2K(\hat{q})+B(1-\hat{q}_y^2)]\theta(\mathbf{q})=iB\frac{\mathbf{q}\times\mathbf{m}}{q^2} , \tag{4.4}$$

where $\mathbf{v}(\mathbf{q})$ and $\theta(\mathbf{q})$ are the Fourier transforms of $\mathbf{v}(\mathbf{x})$ and $\theta(\mathbf{x})$, and $K(\hat{q})=K\hat{q}_\perp^2+K_2\hat{q}_x^2$, where $\hat{q}_i^2=q_i^2/q^2$ ($i=x,y,\perp$). The linearized elastic free energy in the presence of dislocations is then[26]

$$F_{el}=\tfrac{1}{2}B\int\frac{d^3q}{(2\pi)^2}\left[\left[\frac{\mathbf{q}\times\mathbf{m}}{q^2}\right]_t^2+\frac{q^2K(\hat{q})-B\hat{q}_y^2}{q^2K(\hat{q})+B(1-\hat{q}_y^2)}\left[\frac{\mathbf{q}\times\mathbf{m}}{q^2}\right]_y^2\right] , \tag{4.5}$$

where t refers to directions perpendicular to the y axis.

For a single screw dislocation of unit strength, with core parallel to the y axis,

$$\mathbf{m}(\mathbf{x})=d\delta(x)\delta(y)\hat{z} ,$$
$$\mathbf{m}(\mathbf{q})=2\pi d\delta(q_z)\hat{z} . \tag{4.6}$$

The strain energy per unit length of a single screw dislocation is, therefore,

$$\epsilon_{screw}=\tfrac{1}{2}Bd^2\int\frac{dq_x dq_y}{(2\pi)^2}\frac{K(\hat{q})}{[q^2K(\hat{q})+B\hat{q}_x^2]}$$
$$=\tfrac{1}{2}Bd^2\int_0^{\xi^{-1}}\frac{qdq}{(2\pi)^2}\int_0^{2\pi}d\gamma\frac{1}{q^2+[B/K(\gamma)]\sin^2\gamma}$$
$$=\frac{Bd^2}{2\pi}\ln(\lambda_2/\xi)+\frac{Bd^2}{8\pi^2}\int d\gamma\ln\left[\frac{K(\gamma)}{K_2\sin^2\gamma}+\frac{\xi^2}{\lambda_2^2}\right] , \tag{4.7}$$

where $K(\gamma)=K\sin^2\gamma+K_2\cos^2\gamma$. When $\lambda_2/\xi\gg1$, the first term in Eq. (4.7) dominates and is identical to the energy of a vortex in a superconductor. The second term is not present in a superconductor. It is, however, perfectly finite and can be absorbed into a redefinition of the core energy. We, therefore, have

$$\epsilon_{screw}=\frac{Bd^2}{(2\pi)}\ln(\lambda_2/\xi)+\epsilon_{core} , \tag{4.8}$$

just as in a superconductor. We should point out here that it is not *a priori* obvious that the dislocation energy per unit length in our model with constrained director should be finite as in a superconductor rather than diverge logarithmically with the sample size as in an xy model. In fact, the energy of an edge dislocation is xy-like and proportional to the log of the sample size.

We can now calculate h_{c1} in the extreme type-II limit. Right at h_{c1}, the dislocations are separated by distances much greater than λ_2 so that interactions between dislocations can be neglected. The Gibbs free energy per unit volume is

$$G/V=l_d^{-1}l_b^{-1}\epsilon_{screw}-h\bar{k}_0$$
$$=l_d^{-1}l_b^{-1}(\epsilon_{screw}-hd) , \tag{4.9}$$

where we used Eq. (3.2) for $\bar{k}_0$. h_{c1} is the value of h for which the energy gained by inserting twist first overcomes the energy cost of creating a dislocation and is determined by $G/V=0$. Therefore,

$$h_{c1}=K_2k_{c1}=\epsilon_{screw}/d \to \frac{Bd}{2\pi}\ln(\lambda_2/\xi)$$
$$=\frac{h_c}{\sqrt{2}\kappa_2}\ln(\lambda_2/\xi) , \tag{4.10}$$

where the last two expressions are valid only in the limit $\lambda_2/\xi\gg1$. This is the exact analog of H_{c1} for an extreme type-II superconductor. For sufficiently large λ_2/ξ, the smectic phase in mean-field theory is always unstable to the TGB state before it becomes unstable to the cholesteric state.

The above calculation of h_{c1} does not determine l_d or l_b, just as the analogous calculation of H_{c1} in a superconductor does not determine the lattice parameters of the Abrikosov flux lattice. To find l_d and l_b, it is necessary to include interactions between dislocations. In superconductors, all vortices are parallel, and their interaction is isotropic and repulsive implying a close-packed triangular lattice for the minimum energy state. In the present case, dislocations in different grain boundaries are not parallel, and the interaction between dislocations is not isotropic. Nevertheless, it should be possible to incorporate dislocation interactions in a systematic way and to calculate l_b and l_d near k_{c1}. We expect that this calculation will produce lock-in states with $\alpha=(q_0l_d)^{-1}$ rational and floating states with α irrational. At this point, we cannot tell to what extent the lock-in states at rational α are of finite measure in the phase diagram.

V. THE UPPER CRITICAL FIELD

The upper critical field h_{c2} is determined by the limit of stability of the cholesteric phase with $\mathbf{n}=\mathbf{n}_0(\mathbf{x})$ given by Eq. (2.2). The condition for stability is that the eigenvalues of the kernel,

$$M(\mathbf{x},\mathbf{x}')=\frac{\delta F_G^0}{\delta\psi^*(\mathbf{x})\delta\psi(\mathbf{x})}$$
$$=[-C\nabla^2+2Ciq_0\mathbf{n}_0(\mathbf{x})\cdot\nabla+Cq_0^2+r]\delta(\mathbf{x}-\mathbf{x}') , \quad (5.1)$$

be positive. The condition $\nabla\cdot\mathbf{n}_0(\mathbf{x})=0$ was used in deriving this equation. The only explicit spatial dependence of the kernel in Eq. (5.1) arises from the x dependence of $\mathbf{n}_0(\mathbf{x})$. Therefore, the eigenfunctions of the operator $\hat{M}$, whose matrix elements in coordinate space are given by Eq. (5.1), are of the form

$$\psi(\mathbf{x})=\phi_{\mathbf{q}_\perp}(\mathbf{x})e^{i\mathbf{q}_\perp\cdot\mathbf{x}} , \quad (5.2)$$

where the vector,

$$\mathbf{q}_\perp=q_\perp(0,\sin\eta,\cos\eta)=q_\perp\mathbf{n}_0(\eta/k_0) , \quad (5.3)$$

has a vanishing x component. When acting on functions with this plane-wave dependence on the transverse components of position, the stability operator reduces to a Mathieu operator,

$$\hat{M}=-C\partial_x^2+C(q_\perp-q_0)^2$$
$$+2Cq_0q_\perp[1-\cos(k_0x-\eta)] . \quad (5.4)$$

This operator is the Schrödinger operator of an electron in a cosine potential. The ratio $(q_0q_\perp/k_0^2)\sim q_0^2/k_0^2$ is a dimensionless measure of barrier height compared to kinetic energy. When this ratio is large, the electron bandwidths are of order $\exp[-\text{const.}\times(q_0/k_0)]$. In a typical cholesteric, $q_0\sim 2\pi/(30\text{ Å})$ and $k_0\sim 2\pi/(3000\text{ Å})$ so that $(q_0/k_0)>10^2$, implying negligibly small bandwidths.

The functions diagonalizing $\hat{M}$ are Bloch functions, which can be expressed as linear combinations of Wannier functions localized about each of the minima, located at $x_{\eta,l}=2\pi l/k_0+\eta/k_0$ with l an integer, of the periodic potential. To leading order in (k_0/q_0), the Wannier functions are simply harmonic-oscillator functions $\phi^n_{\mathbf{q}_\perp}(x)$ centered at $x_{\eta,l}$. The lowest energy (unnormalized) wave function is

$$\phi^0_{\mathbf{q}_\perp}(x)=\exp[-\tfrac{1}{2}\bar{\xi}^{-2}(x-x_{\eta,l})^2]\equiv\phi(x-x_{\eta,l}) , \quad (5.5)$$

where $\bar{\xi}^{-2}=\sqrt{q_0q_\perp}\,k_0\approx q_0k_0$. Note that the position of the maximum of the Wannier functions is determined by the direction of spatial modulation in the y,z plain. One can see from Eq. (5.3) that these wave functions, as expected, describe fluctuations towards a phase in which the direction of spatial modulation is parallel to the local director. Corrections to the harmonic-oscillator states can be calculated in a systematic power series in (k_0/q_0) by including anharmonic terms in the expansion of the cosine potential about its minima. Off-diagonal matrix elements of the Mathieu Hamiltonian between states localized in different anharmonic wells are exponentially small in (q_0/k_0). These exponentially small terms, which we neglect, lead to lock in of α to rational (or commensurate) values p/q (see Sec. VI).

The eigenvalues of the harmonically approximated kernel associated with the nth harmonic-oscillator wave functions $\phi^n_{\mathbf{q}_\perp}$ are

$$\epsilon_n(k_0,\mathbf{q}_\perp)=C[(2n+1)\bar{\xi}^{-2}+(q_\perp-q_0)^2+r/C] . \quad (5.6)$$

Note these eigenvalues depend only on the magnitude of $\mathbf{q}_\perp$ and not on its direction. We will be particularly interested in these eigenvalues in the vicinity of their minimum. The value of $q_\perp$ that minimizes ϵ_n is

$$q_{\perp n}=q_0[1-\tfrac{1}{4}(2n+1)(k_0/q_0)+O(k_0^2/q_0^2)] . \quad (5.7)$$

The ground-state energy $\epsilon_0(k_0,\mathbf{q}_\perp)$ evaluated at the minimum with respect to $\mathbf{q}_\perp$ passes through zero for $r<0$ when

$$\bar{\xi}^{-2}=\sqrt{q_0q_\perp}\,k_0=|r|/C=\xi^{-2} \quad (5.8)$$

or when k_0 is equal to

$$k_{c2}=h_{c2}/K_2=q_0^{-1}(-r/C)[1+O(k_0/q_0)] . \quad (5.9)$$

The coefficient of the order (k_0/q_0) correction term depends on anharmonic corrections to the harmonic approximation. The eigenvalues Eq. (5.6) can now be expanded about $k_0=k_{c2}$, $q_\perp=q_{\perp n}$:

$$\epsilon_n(k_0,q_\perp)\approx C\xi^{-2}\{(2n+1)[(k_0-k_{c2})/k_{c2}]$$
$$+2n+\xi^2(q_\perp-q_{\perp n})^2\} . \quad (5.10)$$

It is clear from this expression that the least stable mode is the $n=0$ mode with energy,

$$\epsilon_0(k_0,q_\perp)=C\xi^{-2}[(k_0-k_{c2})/k_{c2}+\xi^2(q_\perp-q_0)^2]$$
$$=C\xi_2^{-2}[1+\xi_2^2(q_\perp-q_0)^2] , \quad (5.11)$$

where

$$\xi_2=\xi[(k_0-k_{c2})/k_{c2}]^{-1/2} \quad (5.12)$$

is the twist lattice correlation length that diverges as $k_0\to k_{c2}$. The limit of stability of the cholesteric phase occurs at $h=h_{c2}=\sqrt{2}\kappa_2h_c$ or equivalently at $k_0=k_{c2}=\sqrt{2}\kappa_2k_c$, which, to lowest order in ξ^{-2}, satisfies $q_0k_{c2}=\xi^{-2}$. The transition from type-I to type-II behavior occurs at $\kappa_2=1/\sqrt{2}$.

VI. THE TGB STATE NEAR h_{c2}

In Sec. V we determined the limit of metastability of the cholesteric phase. In this section, we will study the TGB phase for $h=h_{c2}^-$. Our analysis follows very closely that of Abrikosov[6,13] for the flux lattice phase in a superconductor just below H_{c2}. We begin by expressing the order parameter as a linear combination of the ground-state wave functions, $e^{i\mathbf{q}_\perp\cdot\mathbf{x}}\phi(x-x_{\eta,l})$ diagonalizing the linearized theory at h_{c2}. In general, one should introduce amplitudes $C_{\eta,l}$ for each η and l. Instead, we use a somewhat restricted ansatz that, as we will show, leads to the rotation of planes we expect in the TGB state. We set

$$\psi(\mathbf{x})=\sum_s C_se^{i\mathbf{q}_\perp^s\cdot\mathbf{x}}\phi(x-x_s) , \quad (6.1)$$

where $\mathbf{q}_\perp^s=[q_0+O(k_0)]\mathbf{n}_0(x_s)$ and $k_0x_s=2\pi\alpha s$ with s an

integer. In this wave function, η and l are determined by the single integer s via $l=[\alpha k_0 s]$ and $\eta=\{2\pi\alpha k_0 x\}$ where $[w]$ is the greatest integer less than or equal to w and $\{w\}$ is the fractional part of w. In general, the coefficients C_s are complex with an amplitude $|C_s|$ and a phase u_s.

It is useful to see how the ansatz of Eq. (6.1) is related to that of Abrikosov for the superconductor. If $\mathbf{q}_\perp^s$ is replaced by its form $(0,q_0 2\pi\alpha s,q_0)=(0,ks,q_0)$ valid for small x_s, then Eq. (6.1) reduces to

$$\psi(\mathbf{x})\sim e^{iq_0 z}\sum_s C_s e^{iksy}\phi(x-x_s)$$
$$\equiv e^{iq_0 z}\psi_{\mathrm{Abr}}(x,y)\ , \tag{6.2}$$

where $\psi_{\mathrm{Abr}}(x,y)$ is the Abrikosov solution for a superconductor. The Abrikosov solution is clearly unacceptable for the liquid crystal because, as illustrated in Fig. 6, it would lead to layer spacings far from the preferred value d of the smectic.

It is easy to see that Eq. (6.1) does in fact produce a TGB lattice of the type described in Sec. III. $|\psi(\mathbf{x})|$ attains its maximum value, corresponding to the greatest degree of smectic ordering, on the planes $\mathbf{x}=(x_s,y,z)$. On these planes, there is a one-dimensional mass density modulation with period d along the direction $\mathbf{n}_0(x_s)$. $|\psi(\mathbf{x})|$ attains its minimum value on the planes $\mathbf{x}=(x_s+\frac{1}{2}l_b,y,z)$ where $l_b=2\pi\alpha/k_0=(k/k_0 q_0)$. Thus, there is a regular sequence of smectic regions with directions of spatial modulation progressing in a helical fashion. The planes of minimum $|\psi(\mathbf{x})|$ are the grain boundaries discussed in Sec. III and illustrated in Fig. 2. One should observe that had we taken a more general linear combination of the eigenfunctions $e^{i\mathbf{q}_\perp\cdot\mathbf{x}}\phi(x-x_{\eta,l})$ than that of Eq. (6.1), then our smectic regions would not be as evenly spaced.

The ansatz of Eq. (6.1) contains the two unspecified lengths, l_b and $l_d=2\pi/k$ introduced in the discussion of the TGB state in Sec. III. There are also two lengths in the Abrikosov ansatz for the superconductor. In that case, the ratio $R=2l_b/l_d=k^2/(\pi k_0 q_0)$ of the two lengths determines the symmetry of the vortex lattice. As shown by Kleinert, Roth, and Autlers[13] (KRA),

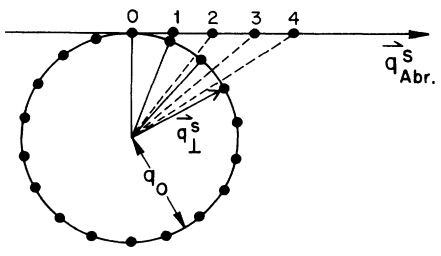

FIG. 6. Vectors $\mathbf{q}_\perp^s$ lying on a circle of radius q_0 compared to the vectors $\mathbf{q}_{\mathrm{Abr}}^s$ that would be used to obtain an Abrikosov lattice of parallel screw dislocations. The vectors $\mathbf{q}_{\mathrm{Abr}}^s$ have a constant x component, and their magnitude increases with increasing s. They are, therefore, unacceptable for creating a low-energy TGB state.

$R=\sqrt{3}$ in the lowest energy triangular vortex lattice state. The values of l_b and l_d at H_{c2} are then determined by $B=H_{c2}=n_v\Phi_0$ where $n_v=l_b^{-1}l_d^{-1}=\xi^{-2}$. In what follows, we will calculate R for the smectic liquid crystal following the procedures of Abrikosov and Ref. 6. In general, R depends on K/K_2. For $K/K_2=0$, we find $R=1.91$, rather than $\sqrt{3}\approx 1.73$. Once R has been determined, l_b can be determined at k_{c2} by $\bar{k}_0=k_{c2}=\pi R/q_0 l_b^2$ [Eq. (3.2)]. For $k_0<k_{c2}$, $\bar{k}_0$ will decrease and l_b increase.

We now turn to the actual minimization procedure used to determine ψ and R for $k_0=k_{c2}^-$. We begin by setting $\theta=k_{c2}x+\delta\theta$ and expanding G [Eq. (2.10)] to lowest order in $\delta\theta$:

$$G=F_G^{00}-\int d^3x\,\delta\theta(\mathbf{x})J_\theta^0+F_G^{NL}+G_F\ , \tag{6.3}$$

where F_G^{00} is F_G^0 evaluated at $\theta=k_{c2}x$ and

$$J_\theta^0=\left.\frac{\delta F_G^0}{\delta\theta}\right|_{\theta=k_{c2}x}$$
$$=-iCq_0(\psi^*\nabla\psi-\psi\nabla\psi^*)\cdot\left.\frac{\delta\mathbf{n}}{\delta\phi}\right|_{\theta=k_{c2}x}\ . \tag{6.4}$$

F_G^{00} is zero for any linear combination (Eq. 6.1) of ground-state wave functions of the linearized theory at $k_0=k_{c2}$. $\delta\theta$ is then determined in terms of J_θ^0 by minimizing Eq. (6.3) with respect to θ. We obtain

$$-(K_2\nabla_x^2+K\nabla_\perp^2)\delta\theta=J_\theta^0\ . \tag{6.5}$$

The solution to this equation is $\delta\theta=k_0'x+\delta\theta'$ where

$$\delta\theta'=-(K_2\nabla_x^2+K\nabla_\perp^2)^{-1}J_\theta^0\ . \tag{6.6}$$

The constant k_0' is chosen to minimize G_F [Eq. (2.11)], i.e., $k_0'=k_0-k_{c2}$ so that $\theta=k_0x+\delta\theta'$. Using $F_G^{00}=0$ and the above expression for $\delta\theta$ in Eq. (6.3), we obtain

$$G=K_2(k_0-k_{c2})\int d^3x\,\nabla_x[\nabla^{-2}K^{-1}(\hat{\nabla})J_\theta^0(\mathbf{x})]$$
$$-\tfrac{1}{2}\int d^2x\,J_\theta^0(\mathbf{x})\nabla^{-2}K^{-1}(\hat{\nabla})J_\theta^0(\mathbf{x})$$
$$+\tfrac{1}{2}g\int d^3x\,|\psi(\mathbf{x})|^4-\tfrac{1}{2}VK_2k_0^2\ , \tag{6.7}$$

where $K(\hat{\nabla})$ was defined in Eq. (4.4). This is the fundamental equation for our analysis of the TGB lattice near h_{c2}.

To proceed with our calculations, we assume, as already discussed, that $k_0/q_0\ll 1$. We further consider only irrational α and ignore any lock in corrections. The restriction to $k_0/q_0\ll 1$ considerably simplifies our expression for J_θ^0. The product $\nabla\psi\cdot(d\mathbf{n}/d\theta)$ produces terms proportional to $\phi(x-x_s)\sin k_{c2}(x-x_s)$. The wave function $\phi(x-x_s)$ restricts $(x-x_s)$ to be less than $\xi=(q_0k_{c2})^{-1/2}$. Thus $k_{c2}(x-x_s)<(k_0/q_0)^{1/2}$, implying that $\sin k_{c2}(x-x_s)$ can be replaced by $k_{c2}(x-x_s)$ to lowest order in k_{c2}/q_0. Using this replacement and the harmonic-oscillator form of $\phi(x)$, we find

$$J_\theta^0=Cq_0\nabla_x|\psi|^2\ . \tag{6.8}$$

This is identical to the expression for the supercurrent in

the Abrikosov calculation.[5,6]

With this approximation, Eq. (6.7) for the free energy becomes

$$G=-\tfrac{1}{2}VK_2k_0^2+C(k_0-k_{c2})\int d^3x\,|\psi(\mathbf{x})|^2 +\tfrac{1}{2}g\int d^3x\,|\psi(\mathbf{x})|^2 \times\left[1-\frac{1}{2\kappa_2^2}\frac{\nabla_x^2}{\nabla_x^2+(K/K_2)\nabla_\perp^2}\right]|\psi(\mathbf{x})|^2 . \tag{6.9}$$

The simple form of the quadratic term results from the fact that the integrals over y and z set $\mathbf{q}_\perp^s=\mathbf{q}_\perp^{s'}$ so that $\nabla_x^2[\nabla_x^2+(K/K_2)\nabla_\perp{}^2]^{-1}\to 1$ when acting on $|\psi(\mathbf{x})|^2$. To put G into its final form, we minimize Eq. (6.9) with respect to the spatial average of ψ^2 at fixed

$$\tilde{\beta}=\frac{1}{[\,|\psi|^2]_{\rm av}} \times\left[|\psi|^2\left[1-\frac{\nabla_x^2}{2\kappa_2^2[\nabla_x^2+(K/K_2)\nabla_\perp^2]}\right]|\psi|^2\right]_{\rm av}, \tag{6.10}$$

where $[A]_{\rm av}=V^{-1}\int d^3x\,A$ denotes the spatial average of A. We find

$$\frac{G}{K_2k_0{}^2V}=-\frac{1}{2}-\frac{1}{\tilde{\beta}K_2}\left[\frac{k_0-k_{c2}}{k_0}\right]^2 . \tag{6.11}$$

We observe that when $K/K_2\to 0$,

$$\tilde{\beta}\to[1-1/(2\kappa_{2_2})][\,|\psi|^4]_{\rm av}/[\,|\psi|^2] \equiv[1-1/(2\kappa_2^2)]\beta , \tag{6.12}$$

and Eq. (6.11) reduces to the Gibbs free energy for a superconductor derived by KRA.[13] The free energy in Eq. (6.11) attains its minimum value at the minimum value of $\tilde{\beta}$ which we calculate below.

We begin our analysis for $K/K_2=0$. Although the free energy [Eq. (6.11)] reduces to the KRA expression in this limit, the value of $R=2l_b/l_d$ does not reduce to the superconducting value of $\sqrt{3}$ because of the different forms for ψ in the two cases. The calculation of $[\,|\psi|^4]_{\rm av}$ requires sums over every set of four vectors $\mathbf{q}_\perp^{s1}$, $\mathbf{q}_\perp^{s2}$, $\mathbf{q}_\perp^{s3}$, and $\mathbf{q}_\perp^{s4}$ such that $\mathbf{q}_\perp^{s1}+\mathbf{q}_\perp^{s2}=\mathbf{q}_\perp^{s3}+\mathbf{q}_\perp^{s4}$. In the Abrikosov case all $\mathbf{q}_\perp$ are colinear so that there is an infinite number of vectors $\mathbf{q}_\perp^{s3}$ and $\mathbf{q}_\perp^{s4}$ contributing to $[\,|\psi|^4]_{\rm av}$ once $\mathbf{q}_\perp^{s1}$ and $\mathbf{q}_\perp^{s2}$ are specified. In the liquid-crystal case, all vectors $\mathbf{q}_\perp^s$ lie on a circle of radius q_0 so that there are only three possible choices for $\mathbf{q}_\perp^{s1}$, $\mathbf{q}_\perp^{s2}$, $\mathbf{q}_\perp^{s3}$, and $\mathbf{q}_\perp^{s4}$. They are

$$\begin{aligned}&(1)\ \mathbf{q}_\perp{}^{s1}=\mathbf{q}_\perp{}^{s3}\ ,\ \ \mathbf{q}_\perp{}^{s2}=\mathbf{q}_\perp{}^{s4}\ ;\\ &(2)\ \mathbf{q}_\perp{}^{s1}=\mathbf{q}_\perp{}^{s4}\ ,\ \ \mathbf{q}_\perp{}^{s2}=\mathbf{q}_\perp{}^{s3}\ ;\\ &(3)\ \mathbf{q}_\perp{}^{s1}=-\mathbf{q}_\perp{}^{s2}\ ,\ \ \mathbf{q}_\perp{}^{s3}=-\mathbf{q}_\perp{}^{s4}\ .\end{aligned} \tag{6.13}$$

When α is irrational, $\mathbf{q}_\perp{}^s=\mathbf{q}_\perp{}^{s'}$ if and only if $s=s'$. In this case, each factor of C_s in $[\,|\psi|^4]_{\rm av}$ is paired with C_s^* so that $[\,|\psi|^4]_{\rm av}$ is a sum of terms with coefficients $|C_{s1}|^2|C_{s2}|^2$ independent of the phase u_s of C_s leading to

$$\beta=\frac{[\,|\psi|^4]_{\rm av}}{[\,|\psi|^2]_{\rm av}^2}=\sqrt{2R}\left[\sum_{r=-\infty}^{\infty}e^{-\pi Rr^2/2}-\tfrac{1}{2}\right] . \tag{6.14}$$

To obtain this result, care must be taken not to double count terms in which $s1=s2=s3=s4$.

The corresponding solution for the superconductor is obtained by using Eq. (6.2) rather than Eq. (6.1) for ψ and by setting $C_s=C_{s+2}$. Minimization with respect to C_0 and C_1 then yields $C_0=\pm iC_1$ and

$$\beta_{\rm Abr}=(R/2)^{1/2}(f_0^2-f_1^2+2f_0f_1) , \tag{6.15}$$

where $f_p=\sum_m\exp[-\pi R(2m+p)^2/2]$. Thus, in the Abrikosov case, there is a single undetermined or free phase u_0 (since $u_1=u_0\pm\pi/2$) whereas in the liquid-crystal case with α irrational, there are an infinite number of phases undetermined by the energy minimization procedure. This result is in agreement with our counting of phason degrees of freedom in Sec. III.

When $\alpha=p/q$ is rational, then $\mathbf{q}_\perp^s=\mathbf{q}_\perp^{s'}$ for $s'=s+tq$ for any integer t. Consequently, there will be terms in $[\,|\psi|^2]_{\rm av}$ and $[\,|\psi|^4]_{\rm av}$ coupling the phases $u_s(\mathbf{x}_\perp)$ and $u_{s+tq}(\mathbf{x}_\perp)$ of dislocation lines in identically oriented grain boundaries (two grain boundaries are identically oriented if the axes of their constituent dislocation lines are parallel). This coupling produces cusplike minima in the free energy $F_F(\alpha)$ at rational α which can cause the TGB phase to be commensurately locked to the cholesteric pitch. A second source of lock-in terms arises from the tunneling corrections to the spectrum of the linear stability operator $\hat{M}$ in Eq. (5.4). When these are included, the least stable modes can no longer be chosen to be the Wannier functions $\phi(x-x_s)$. Instead one must work with Bloch functions, $\phi_{\mathbf{k}}=\sum_t e^{i\mathbf{k}\cdot\mathbf{x}_{s+tq}}\phi(x-x_{s+tq})$, near the bottom of the band (i.e., near $\mathbf{k}\approx 0$). Structures incommensurate with respect to the cholesteric pitch contain $\mathbf{k}\neq 0$ components (suppressed due to the finite stability bandwidth) or contain overlapping Wannier functions. The latter would be suppressed by nonlinear terms in the free energy. Both of these lock-in effects involve the overlap between $\phi(x-x_s)$ and $\phi(x-x_{t+sq})$ and, therefore, are exponentially small in k_0/q_0. Whether or not lock in occurs, the number of independent phases is less than or equal to q, in agreement with our counting in Sec. III.

In Fig. 7 we plot $\beta(R)$ together with $\beta_{\rm Abr}(R)$ for $K/K_2=0$. The minimum value of β is 1.17 and occurs at $R_{\rm min}=1.91$ and that of $\beta_{\rm Abr}$ at $R_{\rm Abr}=\sqrt{3}$. The fact that $R_{\rm min}>\sqrt{3}$ has a simple interpretation: Because dislocation lines in neighboring grain boundaries are not parallel, they must either interpenetrate, which is energetically costly, or they must separate as much as possible. This causes the interplanar spacing l_b, and thus $R_{\rm min}$ to increase above that for the Abrikosov lattice. $\beta(R)$ has only one minimum whereas $\beta_{\rm Abr}(R)$ has two. This is because the cholesteric with chiral symmetry lacks the $x\to y$, $y\to -x$ invariance of the rotationally isotropic superconductor. A minimum at small R in a cholesteric

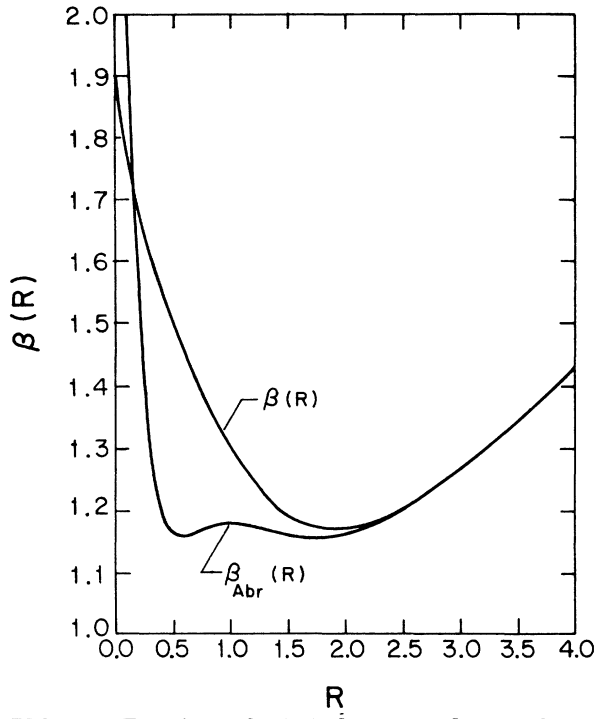

FIG. 7. Functions $\beta_{\rm Abr}(R)$ [Eq. (6.15)] and $\beta(R)$ for $K/K_2=0$ [Eq. (6.14)]. $\beta_{\rm Abr}(R)$ has two minima at $R_{\rm min}=1/R_{\rm min}=\sqrt{3}\approx 1.73$. $\beta(R)$ has a single minimum at $R_{\rm min}=1.91>\sqrt{3}$.

would correspond to a lattice of highly interpenetrating flux lines.

When $K/K_2=0$, $\beta(R)$ has a single positive minimum, and the TGB state is stable when $h_{c1}<h<h_{c2}$ and $\kappa_2>1/\sqrt{2}$. The condition for stability of the TGB phase as a function of κ_2 is identical to the condition that the system be type-II, i.e., $h_{c2}>h_c$. Now, consider the situation for $K/K_2>0$. By inserting Eq. (6.1) into Eq. (6.10), we obtain the following generalization of Eq. (6.14):

$$\tilde{\beta}=\sqrt{2R}\left[1-\frac{1}{2\kappa_2^2}\right]\left[\sum_{s=-\infty}^{\infty}[1+J_s(R)]e^{-\pi Rs^2/2}-\tfrac{1}{2}\right], \tag{6.16}$$

where

$$J_s=\left[1-\frac{1}{2\kappa_2^2}\right]^{-1}\times\int\frac{dy}{\sqrt{2\pi}}e^{-y^2/2}\left[1-\frac{1}{2\kappa_2^2}\frac{y^2}{y^2+\pi Rs^2K/K_2}\right]. \tag{6.17}$$

We see that as $K/K_2\to 0$, $\tilde{\beta}(R)\to[1-(1/2\kappa_2^2)]\beta(R)$ where $\beta(R)$ is given in Eq. (6.14). In Fig. 8(a) we plot $\tilde{\beta}(R)$ for $K/K_2=0.0$, 0.2, 3.0, and 10^4 with $\kappa_2=0,80>1/\sqrt{2}$. As K/K_2 increases from zero, $R_{\rm min}$ increases from 1.91 to 2.94. Physically, this is because increasing the grain boundary spacing l_b relative to the intraplanar dislocation spacing l_d reduces the twist of the TGB phase. In Fig. 8(b) we plot $\tilde{\beta}(R)$ with

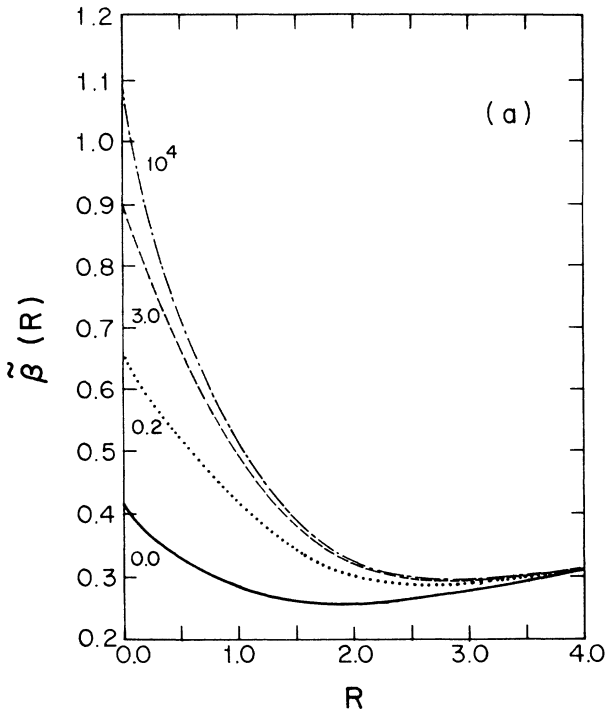

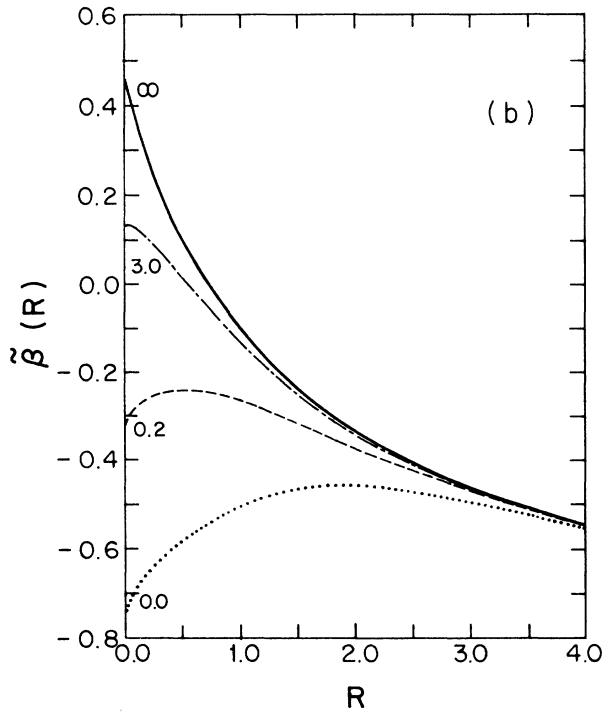

FIG. 8. $\tilde{\beta}(R)$ for fixed κ_2 and $K/K_2=0$, 0.2, 3.0, and 10^4. (a) $\kappa_2=0.80>1/\sqrt{2}$. The lattice spacing ratios $R_{\rm min}$ for the values of K/K_2 listed above are, respectively, 1.9, 2.7, 2.8, and 2.9. Note that l_b/l_d increases by 50% as the ratio of the bend to splay rigidity tends to infinity. (b) $\kappa_2=0.60<1/\sqrt{2}$. $\tilde{\beta}(R)$ is not positive definite indicating an amplitude instability of the large R structures to the spatially uniform smectic phase. If $\tilde{\beta}(R)$ had a positive minimum at $R\neq 0$, there would be a metastable Abrikosov structure even when $\kappa_2<1/\sqrt{2}$. No evidence for such a structure was found.

$\kappa_2=0.600<1/\sqrt{2}$. Here we see that, except for $R<0.5$, $\tilde{\beta}(R)$ is always negative. That $\tilde{\beta}(R)$ is negative for some R indicates that the TGB phase is absolutely unstable with respect to the smectic phase. We also note that there are no local minima of $\tilde{\beta}(R)$ at nonzero R with positive $\tilde{\beta}(R)$. Had such a minima occurred, it would have indicated the existence of a metastable TGB phase even when $\kappa_2<1/\sqrt{2}$.

VII. X-RAY SCATTERING

X-ray scattering is usually our most powerful probe of structure. In this section we will discuss x-ray scattering, both from the TGB state and from the cholesteric state for h just above h_{c2}. The x-ray scattering intensity $I(\mathbf{q})$ at scattering vector $\mathbf{q}$ is proportional to the Fourier transform of the density-density correlation function. We need only be concerned with scattering from $\delta\rho(\mathbf{x})$ [Eq. (2.5)] so that

$$I(\mathbf{q})=\frac{1}{V}\int d^3x\int d^3x'\langle\delta\rho(\mathbf{x})\delta\rho(\mathbf{x}')\rangle e^{-i\mathbf{q}\cdot(\mathbf{x}-\mathbf{x}')}\ . \quad (7.1)$$

As shown in Fig. 2, we choose the x axis to be parallel to the cholesteric pitch axis and the director to lie in the (y,z) plane. This implies that the local smectic planes contain lines parallel to the x axis and have normals in the (y,z) plane. As a reference, it is useful to note that in the absence of twist, $I(\mathbf{q})$ would exhibit two diffuse spots in the nematic phase and two Bragg peaks in the smectic phase at $\mathbf{q}=q_0\mathbf{n}_0$ where $\mathbf{n}_0$ is in the (y,z) plane. Twist introduces an ensemble of smectic layer normals leading to a distribution of directions of high-intensity scattering in the (y,z) plane.

In the cholesteric phase, $\langle\psi(\mathbf{x})\rangle=0$, and $I(\mathbf{q})$ is proportional to the Fourier transform of the $\psi^*-\psi$ correlation function, which in the harmonic, zero bandwidth approximation is

$$\chi(\mathbf{x},\mathbf{x}')=\langle\psi(\mathbf{x})\psi^*(\mathbf{x}')\rangle=\sum_{n,l}\int\frac{d^3q}{(2\pi)^3}A_n^{-1}(\mathbf{q}_\perp)\frac{\phi^n_{\mathbf{q}_\perp,l}(x)\phi^{n*}_{\mathbf{q}_\perp,l}(x')}{\epsilon_n(k_0,q_\perp)}e^{i\mathbf{q}_\perp\cdot(\mathbf{x}-\mathbf{x}')}\ , \quad (7.2)$$

where $A_n(\mathbf{q}_\perp)=\int dx\,|\phi^n_{\mathbf{q}_\perp,l}(x)|^2$ is the normalization factor for the nth harmonic oscillator wave function. Fourier transformation of Eq. (7.2) is straightforward. When $k_0\approx k_{c2}$, the $n=0$ mode dominates, and we obtain,

$$I(\mathbf{q})=2\frac{k_0\bar{\xi}}{\sqrt{\pi}}\frac{e^{-q_x^2\bar{\xi}^2}}{C\xi^{-2}[(k_0-k_{c2})/k_{c2}+\xi^2(q_\perp-q_0)^2]}\ . \quad (7.3)$$

The denominator in this equation is simply $\epsilon_0(k_0,q_\perp)$ [Eq. (5.10)]. As $k_0\to k_{c2}{}^+$, $\epsilon_0(k_0,q_\perp)\to 0$ on a ring of radius q_0, whereas $\bar{\xi}\approx(q_0k_{c2})^{-1/2}$ remains finite. As a function of $q_\perp$ at constant q_x, the x-ray scattering profile is a Lorentzian centered at $q_\perp=q_0$ with halfwidth $\xi^{-1}[(k_0-k_{c2})/k_{c2}]^{1/2}$ that tends to zero as $k_0\to k_{c2}$. As a function of q_x at constant $q_\perp$, the profile is a Gaussian with width $\bar{\xi}^{-1}\approx(q_0k_{c2})^{-1/2}$ that remains finite as $k_0\to k_{c2}$. Thus, there is strong scattering on an anisotropic circular torus of principal radius q_0 with width proportional to $(k_0-k_{c2})^{1/2}$ and height $\bar{\xi}^{-1}$ as shown in Fig. 4. This form should be contrasted to the approximate square root of a Lorentzian line shape in $q_\perp$ obtained by powder averaging[27] the scattering intensity of a nematic over directions of $\mathbf{n}_0$ in the (y,z) plane. In such an average, both the height and width of the scattering torus go to zero at the NA transition. Mosaicity of the director in the x direction, would, however, lead to a Gaussian line shape in the q_x direction with nonzero height at the transition. It, therefore, seems likely that $q_\perp$ rather than q_x scans will be the best probes of an approach to the TGB state from the cholesteric state. Away from h_{c2}, the higher harmonic-oscillator states ($n>0$) in Eq. (7.2) contribute to $I(\mathbf{q})$ and broaden its peaks.

In the TGB state, $\langle\psi(\mathbf{x})\rangle$ is nonzero, and there are Bragg scattering peaks in $I(\mathbf{q})$. The Fourier transform of $\langle\delta\rho(\mathbf{x})\rangle=\langle\psi(\mathbf{x})\rangle+\langle\psi^*(\mathbf{x})\rangle$ follows from Eq. (6.1):

$$\langle\delta\rho(\mathbf{q})\rangle=\sqrt{2\pi}\xi\sum_s e^{-q_x^2\xi^2/2}e^{-iq_xx_s}(2\pi)^2\{C_s\delta^{(2)}[\mathbf{q}_\perp-q_0\mathbf{n}_0(x_s)]+C_s^*\delta^{(2)}[\mathbf{q}_\perp+q_0\mathbf{n}_0(x_s)]\}\ . \quad (7.4)$$

The final form of $\langle\delta\rho(\mathbf{q})\rangle$ resulting from the sum over s in the above expression depends on whether α is rational or irrational. If $\alpha=p/q$ is rational, we assume $C_s=C_{s+q}$, and set $s=jq+K$ where $0\le j\le N_j$ and $0\le K\le q-1$ where $N_j=(L_x/2\pi)(k_0/q)$ is the number of q-plane unit cells in a sample of length L_x. The sum over j of $e^{-iq_xx_s}$ is then a sum of Kronecker deltas of strength N_j at q_x equal to multiples of k_0/p. Therefore, when $\alpha=p/q$ is rational,

$$\langle\delta\rho(\mathbf{q})\rangle=(2\pi)^{5/2}\left[\frac{k_0\xi}{p}\right]\sum_{J,K}\{e^{-q_x^2\xi^2/2}e^{-i2\pi JK/q}\delta(q_x-Jk_0/p)[C_K\delta^{(2)}(\mathbf{q}_\perp-\mathbf{q}_\perp{}^K)+C_K^*\delta^{(2)}(\mathbf{q}_\perp+\mathbf{q}_\perp{}^K)]\}\ , \quad (7.5)$$

where $\mathbf{q}_\perp{}^K=q_0\mathbf{n}_0(x_K)$. This equation is valid both for q even and q odd. However, when q is even (p is then necessarily odd), $\mathbf{q}_\perp{}^{K+q/2}=-\mathbf{q}_\perp{}^K$, and

$$\langle\delta\rho(\mathbf{q})\rangle=(2\pi)^{5/2}\left[\frac{k_0\xi}{p}\right]\sum_{J=-\infty}^{\infty}\sum_{K=0}^{q-1}[e^{-i2\pi JK/q}(C_K+C^*_{K+q/2}e^{-i\pi J})e^{-q_x^2\xi^2/2}\delta(q_x-Jk_0/p)\delta(\mathbf{q}_\perp-\mathbf{q}_\perp{}^K)]\ . \quad (7.6)$$

When $C_K = C^*_{K+q/2}$, there is destructive interference, and only terms with J even survive in the above sum. The scattering intensity, $V^{-1}|\langle\delta\rho(\mathbf{q})\rangle|^2$ does not contain the phase information in $\langle\delta\rho(\mathbf{q})\rangle$. $I(\mathbf{q})$ contains delta function spots equally spaced around rings in the $q_y - q_z$ plane for each $q_x = Jk_0/p$. If q is odd, there are $2q$ spots in each ring; if q is even, there are q spots. We find

$$I(\mathbf{q}) = (2\pi)^2 \left[\frac{k_0\xi}{p}\right]^2 \sum_{J=-\infty}^{\infty} \sum_{K=0}^{2q-1} |C_K|^2 e^{-q_x^2\xi^2} \delta(\mathbf{q}-\mathbf{G}^o_{J,K}) , \quad q \text{ odd}$$

$$I(\mathbf{q}) = (2\pi)^2 \left[\frac{k_0\xi}{p}\right]^2 \sum_{J=-\infty}^{\infty} \sum_{K=0}^{q-1} |C_K + C^*_{K+q/2} e^{-i\pi J}|^2 e^{-q_x^2\xi^2} \delta(\mathbf{q}-\mathbf{G}^e_{J,K}) , \quad q \text{ even} \tag{7.7}$$

where

$$\mathbf{G}^o_{J,K} = (Jk_0/p, \mathbf{q}_\perp^{K/2}) , \quad K = 0,1,\ldots,2q-1$$
$$\mathbf{G}^e_{J,K} = (Jk_0/p, \mathbf{q}_\perp^{K}) , \quad K = 0,1,\ldots,q-1 . \tag{7.8}$$

As required, $I(\mathbf{q})$ is invariant under $\mathbf{q} \rightarrow -\mathbf{q}$.

When α is irrational, the phases u_s of the amplitudes C_s are not energetically fixed as discussed in Sec. VI. The average density $\langle\rho(\mathbf{x})\rangle$ depends on all of the phases u_s just as it depends on all of the complex amplitudes C_K, $K = 0,1,\ldots,q-1$ when α is rational. When $C_s = C$ for all s, we find

$$\langle\delta\rho(\mathbf{q})\rangle = 2(2\pi)^{3/2} \left[\frac{k_0\xi}{q_0\alpha}\right] C \sum_{J=-\infty}^{\infty} \sum_{K=-\infty}^{\infty} e^{-q_x^2\xi^2/2} e^{-2iK\eta} \delta(q_\perp - q_0)\delta(q_x - Jk_0/\alpha - 2Kk_0) , \tag{7.9}$$

where η is the angle of $\mathbf{q}_\perp$. Although $\langle\delta\rho(\mathbf{q})\rangle$ depends on the phases u_s, the scattering intensity $I(\mathbf{q})$, when α is irrational and $|C_s| = |C|$, does not. In this case, we find

$$I(\mathbf{q}) = 2(2\pi)^2 \frac{k_0\xi^2}{\alpha q_0} |C|^2 e^{-q_x^2\xi^2} \delta(q_\perp - q_0) . \tag{7.10}$$

Thus when α is irrational, there is scattering of uniform intensity on an infinitely thin cylinder of radius q_0 and height ξ^{-1}.

The scattering intensity from the TGB state is restricted to a cylinder of radius q_0 and height ξ^{-1}. There are no higher harmonics because there is only a single mass density wave in our low-temperature smectic state. It is interesting to see how our expressions for $I(\mathbf{q})$ would be modified in a model with higher Fourier components in the smectic phase. We, therefore, consider a model system (depicted in Fig. 2) in which the smectic layers between grain boundaries are well developed and in which the directions of the normal to the smectic layers undergo an abrupt rotation through an angle $2\pi\alpha$ at each grain boundary. In this case, the position of a mass point on the tth layer in the region between grain boundary s and $s+1$ is

$$\mathbf{x}_{s,t}(\zeta_1,\zeta_2) = (x_s + \zeta_1)\hat{x} + td\,\mathbf{n}_0(x_s) + \zeta_2 \mathbf{e}_\perp(x_s) , \tag{7.11}$$

where $\mathbf{e}_\perp(x_s) = (0, \cos k_0 x_s, -\sin k_0 x_s)$, $-l_b/2 < \zeta_1 < l_b/2$, and $-\infty \le \zeta_2 \le \infty$. When α is rational, the x-ray scattering intensity from this structure depends on whether q is odd or even. If q is odd, there are Bragg peaks at $(Jk_0/p, I\mathbf{q}_\perp^{K/2})$ for I and J arbitrary integers and $K = 0, 1, \ldots, 2q-1$. For q even, there are Bragg peaks at $(J'k_0/p, I\mathbf{q}_\perp^{K})$ for I an arbitrary integer, J' and *even* integer, and $K = 0,1,\ldots,q-1$. Thus, for this ideal structure, $C_K = C^*_{K+q/2}$ [Eqs. (7.4) and (7.6)]. The Bragg peaks for α rational, therefore, are at the intersection of the spokes of wheels and circles of radius Iq_0 in planes perpendicular to the q_x axis as shown in Fig. 9. When α is irrational, there are Bragg cylinders of radius Iq_0.

Bragg scattering from any material occurs at points on a reciprocal lattice consisting of linear combinations with integer coefficients of vectors in some basis. Arbitrary linear combinations of the vectors $\mathbf{G}^o_{J,K}$ and $\mathbf{G}^e_{J,K}$ generate reciprocal lattices with S-fold rotational symmetry with $S = 2q$ for q odd and $S = q$ for q even. If $S = 2$, 4, or 6, the resultant reciprocal lattice has crystallographic symmetry with a shortest length vector. For any other S, the lattice has quasicrystallographic symmetry[14–16] with no shortest length vector and vectors densely distributed in reciprocal space. The most familiar quasicrystal reciprocal lattice is that with tenfold symmetry[14,15] generated by Penrose tilings[28] of the plane. The general properties of $2d$ lattice with S-fold symmetry and of $3d$ lattices with S-fold screw axes are discussed in Ref. 17. Quasicrystal reciprocal lattices have colinear wave vectors with relatively irrational magnitudes and are a special class of the general class of incommensurate lattices. Thus, even if α is rational, the TGB state can be incommensurate in the (y,z) plane.

In general, one would expect scattering on all symmetry-allowed points in the reciprocal lattice. In the case of the TGB state below k_{c2}, there is scattering only on the vectors $G^a_{J,K}$ $(a = e,o)$ because of the existence of only a single Fourier component of the mass density in the low-temperature smectic-A phase. In the more general model with an infinite number of Fourier com-

ponents in the smectic phase, scattering occurs only at the intersections of spokes of a wheel and circles of radius Iq_0. Thus neither of the ideal TGB structures shows scattering on a dense set of spots in reciprocal space as would be expected on the basis of their high rotational symmetry. Presumably, these ideal structures are unstable with respect to distortions with wavelengths of other vectors in the quasicrystal reciprocal lattice. If the amplitudes of these distortions are small, then the scattering intensity would be approximately that shown in Fig. 9 with additional light spots at other reciprocal lattice vectors. It is unlikely that chiral doped smectics with a single mass density wave in the smectic-A phase will ever show any evidence for this behavior. Bilayer and frustrated smectics[29] with two or more well-developed mass density waves might, however.

It is interesting to contrast the scattering pattern from a TGB state with fivefold symmetry with that of a Penrose tiling with the same rotational symmetry. In the former case, as we have seen, there are Bragg peaks at the intersections of spokes of wheel and circles of radius Iq_0. In the latter case, there are Bragg peaks at all vectors $\mathbf{G}$ in the reciprocal lattice, but their intensities[14,30] fall off as the inverse square of a vector $\mathbf{G}^{\perp}$ associated with $\mathbf{G}$. Thus the distribution of visible Bragg peaks is far more uniform in the Penrose than in the TGB case.

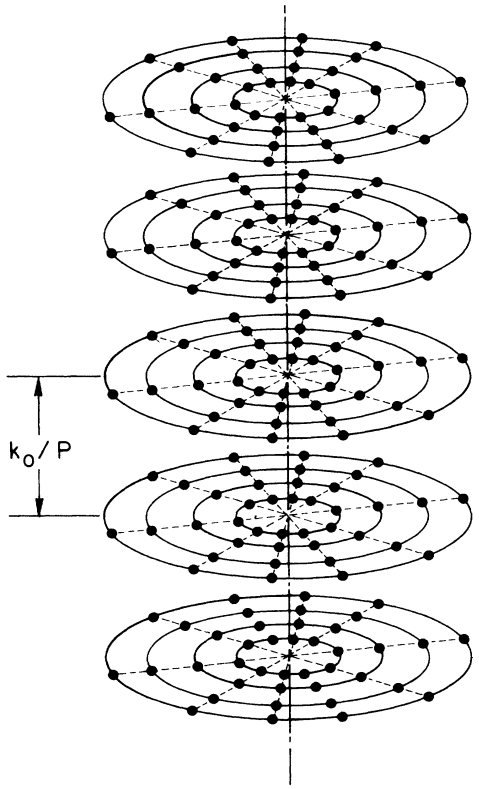

FIG. 9. This figure illustrates the positions of Bragg peaks in scattering from the well-developed TGB state illustrated in Fig. 2 and described by Eq. (7.11) for α rational and $q=5$. At each $q_x=Jk_0/p$ with J an integer, there are Bragg peaks at the intersection of rings of radius Iq_0 (I = 1,2,...) and the ten equally spaced spokes of a wheel. A similar set of Bragg peaks results when $q=10$. In this case, there are Bragg peaks on rings with $q_x=2Jk_0/p$.

As a final observation, we note that there could be terms in the free energy favoring lock in into structures with crystallographic symmetry with possibly very large unit cells. Thus the phase diagram as a function of T and h could be very complex indeed with regions of irrational α and locking regions with rational α divided into subregions with crystallographic and quasicrystallographic symmetry as sketched in Fig. 3.

VIII. DISCUSSION

In this article, we have studied the analog of the Abrikosov vortex state in smectic liquid crystals consisting of, or doped with, chiral molecules favoring a high-temperature cholesteric phase. We found that this state (the TGB state) consists of a regular array of twist grain boundaries composed of parallel screw dislocations as illustrated in Fig. 2. In our analysis, we used a covariant, constrained version of the de Gennes–Frank free energy in which the director, confined to planes perpendicular to the cholesteric pitch axis, is parametrized by a single variable θ. We calculated in mean-field theory the thermodynamic, lower, and upper critical fields h_c, h_{c1}, and h_{c2} and showed that the TGB state in type-II smectics is stable for $h_{c1}<h_c<h_{c2}=\sqrt{2}\kappa_2 h_c$ where κ_2 is the twist Ginzburg parameter. We calculated the x-ray scattering intensity in the cholesteric phase near h_{c2} and in the TGB state for both rational and irrational values of the parameter α measuring the angle of rotation between the axes of screw dislocations in adjacent grain boundaries.

Our analysis is based on a mean-field theory of the simplest possible model, and it is important to know how what we have neglected might affect our results. First, by constraining the director to lie in a plane, we have neglected the Landau-Peierls fluctuation destruction of long-range order in both the cholesteric[21] and smectic phases.[31] We do not believe that removal of this constraint will qualitatively alter our results, but this assertion should be checked. Second, we did not treat exponentially small terms in the free energy contributing when α is rational. These terms will presumably lead to regions of nonzero measure in the $T-h$ phase diagram with α rational. Within these regions, there is the further possibility of lock in to periodic crystal rather than quasicrystal lattices. Third, and most important, we neglected fluctuations in our mean-field analysis. At one level the effects of fluctuations appear to be benign. Critical fluctuations in the vicinity of the NA critical point at $h=0$ lead to scaling of the Gibbs free-energy density $G/V=r^{d\nu}\tilde{g}(h/r^{(d-2)\nu})$ where d is the spatial dimension and ν is the correlation length exponent (we ignore here the possible anisotropy of ν). The correlation length and bend elastic constants obey similar scaling laws: $\xi=r^{-\nu}Y(h/r^{(d-2)\nu})$ and $K_2=r^{-(4-d)\nu}W(h/r^{(d-2)\nu})$. From this, one predicts that both h_c and h_{c2} are proportional to $r^{(d-2)\nu}$ rather than r. Indeed, recent measurements[32] of H_{c2} in extreme type-II high T_c superconduc-

tors are consistent with this scaling analysis. Thus, $\bar{k}_0 = h/K_2$ decreases as $hr^{(4-d)\nu}$ for $h \ll r^{(d-2)\nu}$ and is proportional to $h^{2/(d-2)}$ for $h \gg r^{(d-2)\nu}$. At h_{c2}, $\bar{k}_0$ should be of order $h_{c2}^{2/(d-2)}$. These considerations imply that there should be a well defined phase boundary in the $h-T$ plane separating the cholesteric and TGB phases. The small value of $\bar{k}_0$ could, however, make it very difficult to distinguish the TGB phase from the smectic phase. A potentially more damaging effect of fluctuations arises because the order parameter correlation function $\chi(\mathbf{q})$ [Eq. (7.3)] diverges on a ring as h_{c2} is approached. As discussed by Brasovskii,[33] such fluctuations lead to a first- rather than a second-order transition. (This transition should be more strongly first order than that predicted[34] for the normal to Abrikosov phase transition in superconductors as a result of fluctuations.) It is thus possible that the first-order upper critical field h'_{c2} is depressed below h_{c1} so that there is a first-order cholesteric–to–smectic-A transition as would be predicted in a type-I system.

In Sec. VI, we calculated x-ray scattering intensities for the cholesteric phase near h_{c2} and the TGB phase for both rational and irrational α. Though there are clear mathematical differences between the ideal scattering intensities in these phases, it will be difficult to distinguish the TGB phase from a powder averaged smectic with some director mosaicity. Optically, the TGB phase will be almost indistinguishable from the cholesteric phase. This is a possible explanation of why there has been no experimental observation of the TGB phase. The director (and hence the index of refraction) in the TGB phase rotates in a helical pattern as it does in the cholesteric phase. There are, however, modulations of the director at wave vectors $\mathbf{G}+\bar{k}_0\hat{x}$ where $\mathbf{G}$ is a low-order integer linear combination of $\mathbf{G}^a_{J,K}$, and one might imagine a light scattering experiment to probe satellites of the fundamental cholesteric Bragg scattering peak at $\bar{k}_0\hat{x}$.

Since the TGB phase might easily be misidentified as a cholesteric, it is possible that experiments to date have identified the line $h_{c1}(T)$ as marking the transition from a cholesteric to a smectic-A phase. It should be pointed out that the mean-field theory presented here predicts that the area in the experimentally accessible part of the $h-T$ plane for $T<T_{NA}$ occupied by the TGB phase represents a significant fraction of the area that might be identified as a cholesteric. To see this, let $h_{\max}$ be the maximum experimentally realizable value of h [$\approx K_2 \times (2\pi/3000\text{Å}) \approx 0.05$ dynes/cm] and let τ_1 and τ_2 be the regions in the experimentally accessible part the $h-T$ plane occupied, respectively, by the TGB and cholesteric phases for $T<T_{NA}$. Let T_1 be the temperature at which the line $h=h_{c1}(T)$ and $h=h_{\max}$ cross and T_2 that at which the lines $h=h_{c2}(T)$ and $h=h_{\max}$ cross. Then τ_1 is the triangle with vertices $(h_{\max},T_1)$, $(h_{\max},T_2)$, and $(0,T_{NA})$, and τ_2 is the triangle with vertices $(h_{\max},T_2)$, $(h_{\max},T_{NA})$, and $(0,T_{NA})$. The entire combined region $\tau_1 \cup \tau_2$ could mistakenly be identified as a cholesteric. It is straightforward to show that the ratio of the area of τ_1 to the area of $\tau_1 \cup \tau_2$ is $[1-(2\kappa_2)^{-1}\ln\kappa_2]$ so that the TGB phase occupies a significant fraction of the region for $T<T_{NA}$ that might be identified as a cholesteric as long as $\kappa_2 - 1/\sqrt{2}$ is not too small or negative.

In conclusion, we predict the possibility of a whole class of incommensurate and quasicrystalline structures in smectic liquid crystals composed of chiral molecules. These TGB phases may be very difficult to observe because they do not have a clean optical or x-ray signature. Nevertheless, because of the unusual properties of the TGB phases, we encourage experimentalists to look for ways to detect them, possibly via the appearance of unusual textures.

ACKNOWLEDGMENTS

The authors are extremely grateful to Jim Sethna for very helpful discussions that aided them in identifying the TGB state. They are also grateful to David Wright and Paul Heiney for useful discussions and suggestions. Both authors acknowledge partial support for this work from the National Science Foundation (NSF) under Grant No. DMR-85-20272. One of us (S.R.) also acknowledges partial support from NSF under Grant No. DMR-85-15063. The other (T.C.L.) is grateful for the hospitality of the Institute for Theoretical Physics at Santa Barbara, where some of this work was done.

[1]For a review of the nematic–to–smectic-A transition, see T.C. Lubensky, J. Chim. Phys. **80**, 31 (1983).

[2]P.G. de Gennes, Solid State Commun. **10**, 753 (1972).

[3]B.I. Halperin and T.C. Lubensky, Solid State Commun. **14**, 997 (1973).

[4]V.L. Ginzburg and L.D. Landau, Zh. Eksp. Teor. Fiz. **20**, 1064 (1950).

[5]P.G. de Gennes, *Superconductivity of Metals and Alloys* (Benjamin, New York, 1966); Michael Tinkham, *Introduction to Superconductivity* (McGraw-Hill, New York, 1975).

[6]A.A. Abrikosov, Zh. Eksp. Teor. Fiz. **32**, 1442 (1957) [Sov. Phys.–JETP **5**, 1174 (1957)].

[7]B.I. Halperin, T.C. Lubensky, and Shang-Keng Ma, Phys. Rev. Lett. **32**, 292 (1974); see also Jing-huei Chen, T.C. Lubensky, and D.R. Nelson, Phys. Rev. B **17**, 4274 (1978).

[8]Chandan Dasgupta and B.I. Halperin, Phys. Rev. Lett. **47**, 1556 (1981); Chandan Dasgupta, *ibid.* **55**, 1771 (1985); J. Phys. (Paris) **48**, 957 (1987).

[9]For review of experiments on liquid crystal structure, see Peter Pershan, *Structure of Liquid Crystal Phases* (World Scientific, Singapore, 1988).

[10]J. Sethna (private communication).

[11]W.L McMillan, Phys. Rev. A **6**, 936 (1972).

[12]T.C. Halsey and D.R. Nelson, Phys. Rev. A **26**, 2840 (1982).

[13]W.H. Kleiner, L.M. Roth, and S.H. Autler, Phys. Rev. **133**, A1226 (1964).

[14]D. Levine and P.J. Steinhardt, Phys. Rev. Lett. **53**, 2477 (1984).

[15]For reviews and pedagogical treatments of quasicrystals, see *Selected Reprints on Quasicrystals,* edited by P.J. Steinhardt and S. Ostlund (World Scientific, Singapore, 1987); C.L. Henley, Comments Condensed Matter Phys. **13**, 59 (1987); *Aperiodic Crystals,* edited by Marco Jaric (Academic, Boston, 1988), Vol. I.

[16]Daniel S. Rokhsar, N. David Mermin, and David C. Wright, Phys. Rev. B **35**, 5487 (1987); Acta Crystallogr., Sect. A **44**, 197 (1988); N. David Mermin, Daniel Rokhsar, and David C. Wright Phys. Rev. Lett. **58**, 2099 (1987).

[17]F.C. Frank, Discuss. Faraday Soc. **25**, 883 (1958).

[18]P.G. de Gennes, *The Physics of Liquid Crystals* (Oxford University, London, 1974); S. Chandrasekhar, *Liquid Crystals* (Cambridge, New York, 1977).

[19]R. Alben, Mol. Cryst. Liquid Cryst. **20**, 231 (1973).

[20]R.S. Pindak, Cheng-Cher Huang, and J.T. Ho, Phys. Rev. Lett. **32**, 43 (1974)

[21]T.C. Lubensky, Phys. Rev. Lett. **29**, 206 (1972).

[22]S. Meiboom, J.P. Sethna, P.W. Anderson, and W.F. Brinkman, Phys. Rev. Lett. **46**, 1216 (1981). It is a trivial exercise to see that the director at the core of a twist dislocation in a smectic without external field such as that of Eq. (2.8) rotates away from the axis of the core in all directions in a double twist configuration.

[23]T.C. Lubensky, J. Phys. (Paris), Colloq. **36**, C1-151 (1975).

[24]See, for example, M.J. Buerger, *Elementary Crystallography* (Wiley, New York, 1956).

[25]T.C. Lubensky, in *Aperiodic Crystals,* edited by Marco Jaric (Academic, Boston, 1988), Vol. I.

[26]G. Grinstein, T.C. Lubensky, and John Toner, Phys. Rev. B **33**, 3306 (1986).

[27]L.J. Matinez-Miranda, A.R. Kortan, and R.J. Birgeneau, Phys. Rev. Lett. **56**, 2264 (1986); K.C. Chu and W.L. McMillan, Phys. Rev. A **14**, 1181 (1987).

[28]R. Penrose, Bull. Inst. Math Appl. **10**, 266 (1974); Martin Gardner, Sci. Am. **236**, 110 (1977).

[29]J. Prost and P. Barois, J. Chim. Phys. **80**, 65 (1983); F. Hardouin, A.M. Levelut, M.F. Achard, and G. Sigaud, *ibid.* **80**, 53 (1983).

[30]V. Elser, Phys. Rev. B **32**, 4892 (1985); Acta Crystallogr., Sect. A **42**, 36 (1985); M. Duneau and A. Katz, Phys. Rev. Lett. **54**, 2688 (1985).

[31]A. Caillé, C.R. Acad. Sci. B **274**, 891 (1972).

[32]Kapitulnik (private communication).

[33]S.A. Brasovskii, Zh. Eksp. Teor. Fiz. **68**, 175 (1975) [Sov. Phys.—JETP **41**, 85 (1975)].

[34]E. Brézin, D.R. Nelson, and A. Thiaville, Phys. Rev. B **31**, 7124 (1985).

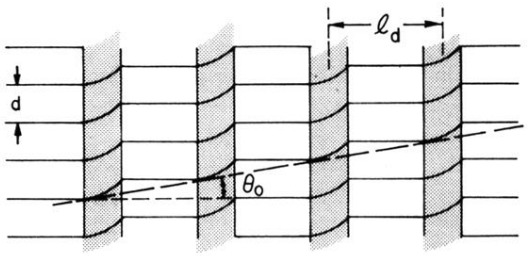

FIG. 3. Schematic representation of a twist grain boundary consisting of parallel twist dislocations (whose cores are darkened) of Burgers vector $d\hat{z}$ separated by distances l_d. The average slope relative to the y axis of the smectic planes in front of the grain boundary is $\frac{1}{2}d/l_d$ while the slope of those behind the grain boundary is $-\frac{1}{2}d/l_d$ leading to a change in angle of normals to smectic planes across the grain boundary of $\Delta\theta = 2\tan^{-1}(\frac{1}{2}d/l_d) \sim d/l_d$.